

AWARD NUMBER: W81XWH-19-1-0363

TITLE: Targeting Neuroendocrine Prostate Cancer with Small-Molecule Drug Conjugates

PRINCIPAL INVESTIGATOR: Dr. Ganesh Raj, MD, PhD

CONTRACTING ORGANIZATION: University of Texas, Southwestern Medical Center  
Dallas, TX

REPORT DATE: October 2021

TYPE OF REPORT: ANNUAL

PREPARED FOR: U.S. Army Medical Research and Development Command  
Fort Detrick, Maryland 21702-5012

DISTRIBUTION STATEMENT: Approved for Public Release; Distribution Unlimited

The views, opinions and/or findings contained in this report are those of the author(s) and should not be construed as an official Department of the Army position, policy or decision unless so designated by other documentation.

# REPORT DOCUMENTATION PAGE

*Form Approved*  
OMB No. 0704-0188

Public reporting burden for this collection of information is estimated to average 1 hour per response, including the time for reviewing instructions, searching existing data sources, gathering and maintaining the data needed, and completing and reviewing this collection of information. Send comments regarding this burden estimate or any other aspect of this collection of information, including suggestions for reducing this burden to Department of Defense, Washington Headquarters Services, Directorate for Information Operations and Reports (0704-0188), 1215 Jefferson Davis Highway, Suite 1204, Arlington, VA 22202-4302. Respondents should be aware that notwithstanding any other provision of law, no person shall be subject to any penalty for failing to comply with a collection of information if it does not display a currently valid OMB control number. **PLEASE DO NOT RETURN YOUR FORM TO THE ABOVE ADDRESS.**

<b>1. REPORT DATE</b> October 2021		<b>2. REPORT TYPE</b> ANNUAL		<b>3. DATES COVERED</b> 01Sep2020 - 31Aug2021	
<b>4. TITLE AND SUBTITLE</b>  Targeting Neuroendocrine Prostate Cancer with Small-Molecule Drug Conjugates				<b>5a. CONTRACT NUMBER</b> W81XWH-19-1-0363	
				<b>5b. GRANT NUMBER</b>	
				<b>5c. PROGRAM ELEMENT NUMBER</b>	
<b>6. AUTHOR(S)</b>  Dr. Ganesh Raj, MD, PhD,  E-Mail:				<b>5d. PROJECT NUMBER</b>	
				<b>5e. TASK NUMBER</b>	
				<b>5f. WORK UNIT NUMBER</b>	
<b>7. PERFORMING ORGANIZATION NAME(S) AND ADDRESS(ES)</b>  University of Texas, Southwestern Medical Center at Dallas				<b>8. PERFORMING ORGANIZATION REPORT NUMBER</b>	
<b>9. SPONSORING / MONITORING AGENCY NAME(S) AND ADDRESS(ES)</b>  U.S. Army Medical Research and Development Command Fort Detrick, Maryland 21702-5012				<b>10. SPONSOR/MONITOR'S ACRONYM(S)</b>	
				<b>11. SPONSOR/MONITOR'S REPORT NUMBER(S)</b>	
<b>12. DISTRIBUTION / AVAILABILITY STATEMENT</b>  Approved for Public Release; Distribution Unlimited					
<b>13. SUPPLEMENTARY NOTES</b>					
<b>14. ABSTRACT</b> Significant progress has been made in understanding the mechanism of action of SphK1 in promoting neuroendocrine progression. NEPC is known as lipid-rich tumor and elevated lipogenic enzymes have been observed in clinical specimens. In cBioPortal, 22% NePC patients have Sphingosine kinase-1 (SphK1) gene amplification; this enzyme produces sphingosine 1-phosphate (S1P) that is a lipid mediator critical for tumor cell growth, survival, and therapeutic resistance. Also, the elevated SphK1 mRNA and protein expression is detected in NEPC cells. By genomic knockout and transcriptomic approaches, the mechanism of action of SphK1 is identified through S1P receptor-MAP kinase pathway leading to the proteasome degradation of RE1-Silencing Transcription factor (REST) that is known as a master repressor of neuroendocrine differentiation. Based on these discoveries, SphK1 is a new therapeutic target for NePC therapy. Indeed, in vitro data support a good potency of SphK1 small molecule inhibitors (FTY720 or SKI-II) in inhibiting NePC growth; the in vivo data is on the way.					
<b>15. SUBJECT TERMS</b>  NONE LISTED					
<b>16. SECURITY CLASSIFICATION OF:</b>			<b>17. LIMITATION OF ABSTRACT</b>  UU	<b>18. NUMBER OF PAGES</b>  31	<b>19a. NAME OF RESPONSIBLE PERSON</b> USAMRDC
<b>a. REPORT</b>  Unclassified	<b>b. ABSTRACT</b>  Unclassified	<b>c. THIS PAGE</b>  Unclassified			<b>19b. TELEPHONE NUMBER</b> (include area code)

# TABLE OF CONTENTS

	<u>Page</u>
1. Introduction	
2. Keywords	
3. Accomplishments	5
4. Impact	
5. Changes/Problems	
6. Products	
7. Participants & Other Collaborating Organizations	
8. Special Reporting Requirements	
9. Appendices	

## DOD Grant Progress Summary

### Descriptive Title:

Drug Conjugates

### Submission Title: Opportunity ID: Opportunity Title: Agency Name:

Targeting Neuroendocrine Prostate Cancer with Small Molecule

PC180542

W81XWH-18-PCRP-IDA

DoD Prostate Cancer, Idea Development Award Dept. of the Army -- USAMRAA

Our overarching goal for this grant was to develop novel small molecule drug conjugates for testing and targeting in novel models of NEPC. We had to change our approach from using Cpd18<sub>14</sub> due to limitations with its target BRN2 being expressed in our NEPC models and change it to an alternate target. We have made significant progress in our studies, including defining two new molecular targets in NEPC- SphK1 and SV2A and overcoming technical barriers towards

Despite COVID-19 restrictions on laboratory staffing, we have made significant progress in 4 distinct areas

1. Defining the importance of the molecular target SphK1 in NEPC (please see draft of manuscript by Cheng-Fan Lee, titled Sphingosine kinase 1 is central to neuroendocrine differentiation of prostate cancer: An opportunity of targeted therapy. We have since published the manuscript [Clin Transl Med. 2022 Feb;12\(2\):e695. doi: 10.1002/ctm2.695.PMID: 35184376](#))
2. Identification of SV2A as a novel target in NEPC (see attached manuscript titled Initial Validation of SV2A-targeted PET Imaging for Noninvasive Assessment of Neuroendocrine Differentiation in Prostate Cancer)
3. Synthesizing SMDC conjugates, overcoming technical barriers towards conjugate synthesis (see attached submitted manuscript by Guan et al, titled Chemically Identical Pair of Small-Molecule Theranostic Conjugates Specific for Prostate Cancer Imaging and Therapy)
4. Developed additional models of NEPC for testing our SMDC conjugates (work ongoing)

## **Accomplishments:**

**Project Area 1a:** Significant progress has been made in understanding the mechanism of action of SphK1 in promoting neuroendocrine progression. NEPC is known as lipid-rich tumor and elevated lipogenic enzymes have been observed in clinical specimens. In cBioPortal, 22% NePC patients have Sphingosine kinase-1 (SphK1) gene amplification; this enzyme produces sphingosine 1-phosphate (S1P) that is a lipid mediator critical for tumor cell growth, survival, and therapeutic resistance. Also, the elevated SphK1 mRNA and protein expression is detected in NEPC cells. By genomic knockout and transcriptomic approaches, the mechanism of action of SphK1 is identified through S1P receptor-MAP kinase pathway leading to the proteasome degradation of RE1-Silencing Transcription factor (REST) that is known as a master repressor of neuroendocrine differentiation. Based on these discoveries, SphK1 is a new therapeutic target for NePC therapy. Indeed, in vitro data support a good potency of SphK1 small molecule inhibitors (FTY720 or SKI-II) in inhibiting NePC growth; the in vivo data is completed and the manuscript was published, *Clin Transl Med.* 2022 Feb;12(2):e695. doi: [10.1002/ctm2.695](https://doi.org/10.1002/ctm2.695). PMID: 35184376

**Project Area 2b:** Identification of SV2A as a novel target in NEPC (see attached manuscript titled Initial Validation of SV2A-targeted PET Imaging for Noninvasive Assessment of Neuroendocrine Differentiation in Prostate Cancer) (submitted to International Journal of Molecular Sciences).

**SV2A holds great potential in nuclear imaging of NED in CRPC.** Our bioinformatic analyses were performed on combined data from three sources: recent reports by Beltran et al, WCMC, and SU2C 2015. We found positive ribonucleic acid (RNA) expression of SV2A in both CRPC-Adeno (n = 147) and NEPC (n = 20), with NEPC being significantly higher. Similar results were observed in another dataset (GSE104786). In addition, we observed an intriguing trend of SV2A expression in a patient-derived xenograft (PDX) model (GSE59986) as adenocarcinoma PCa (AdPC) was progressing to NEPC after castration: the SV2A expression was maintained at a relatively stable and low level within 12 weeks post castration until the emerging of the terminally differentiated NEPC resulting in a drastic increase. Furthermore, we found that the frequency of SV2A gene amplification in metastatic CRPC and NEPC samples (32%, dataset by Beltran *et al.* was markedly higher than that in AdPC samples (2.2%, TCGA Firehose Legacy dataset). As anticipated, NEPC samples also exhibit significant elevation of SV2A from two separate studies. Taken together, SV2A expression is significantly elevated in NEPC.

**Increase in SV2A protein expression with NED development:** Prompted by the encouraging results from the bioinformatic analyses, we did a comparative assay of SV2A protein expression in multiple PCa cell lines, including androgen-responsive AdPC cell line (LNCaP), androgen-responsive CRPC cell line (22Rv1), androgen- negative CRPC-NE & NEPC cell line (PC-3, DU145, and NCI-H660. All cell lines were obtained from the ATCC with frequent authentication and mycoplasma- negative screening. As expected, CRPC-NE and NEPC cell lines presented markedly higher SV2A expressions than AdPC cell lines. Specifically, NCI-H660 had about 23-fold higher SV2A expression than 22Rv1. SV2A is still detectable in AdPC cell lines, indicating the early coexistence of NED to develop NED upon treatment. We were able to obtain and analyze a limited number of CRPC and NEPC patient tissue samples. SV2A showed strong staining in NEPC samples and varied in CRPC samples, which was like the patterns of SYP. In contrast, SSTR2 also varied in CPRC but its expression was lost in NEPC. Altogether, the data supports the detection of NED in CRPC via SV2A.

To determine the location of SV2A in PCa cells, we extracted cell membrane and cytoplasmic fractions from multiple PCa cell lines. The subcellular fractionation WB demonstrated the SV2A presence in both membrane and cytoplasm. NCI-H660 showed dominating location at cell membrane. Of note, we observed that the membrane-bound SV2A isoform possesses a higher molecular weight than its cytoplasm counterpart, perhaps indicative of its higher extent of post-translational modifications. Clearly, these results further suggest the *in vivo* accessibility of SV2A protein to exogenous radioligands.

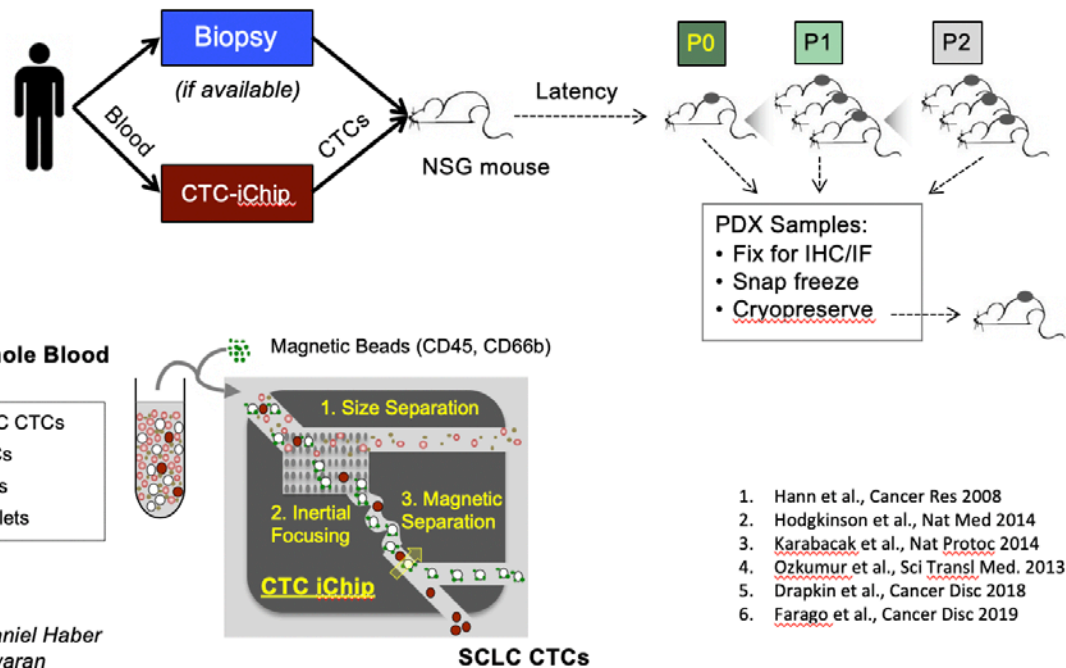
**SV2A-specific NEPC xenograft tumor detection with <sup>18</sup>F-SynVesT-1 PET imaging:** Although <sup>18</sup>F-SynVesT-1 is a typical neuroimaging tracer, we could perform a pilot PET/CT imaging study with it in male SCID NOD micebearing NCI-H660 tumors. The SV2A<sup>+</sup> NCI-H660 tumor could be clearly visualized within 1 hr post-injection (p.i.). The quantitative data indicated that the tumor uptake was consistently higher than that in muscle starting from 10 min p.i. The tumor uptake maintained steady within 1 hr p.i., peaked at  $0.70 \pm 0.14$  %ID/g and then gradually decreased to  $0.29 \pm 0.04$  %ID/g at 4 h p.i. (**Fig. 3B**). To confirm the SV2A imaging specificity, we co-injected excess of <sup>19</sup>F-SynVesT-1 cold ligand for SV2A blockade and observed significantly reduced NCI-H660 tumor uptake from  $0.70 \pm 0.14$  %ID/g to  $0.25 \pm 0.03$  %ID/g ( $p = 0.025$ ). As anticipated, high accumulation in both liver and brain due to its neuroimaging design (high lipophilicity). By time, activity starts to be cleared out of the mice via

urination, indicating tracer instability outside the brain. We were also able to compare the PET imaging of PSMA-11, and  $^{68}\text{Ga}$ -DOTATATE in DU145 tumor bearing mice. Apparently, this NEPC tumor could be successfully detected by SV2A-PET but not the PSMA- or SSTR-PET. Collectively, SV2A was proved a promising target to noninvasively detect NED, while it urges for the oncological version of SV2A-specific radioligands.

Manuscript with figures attached.

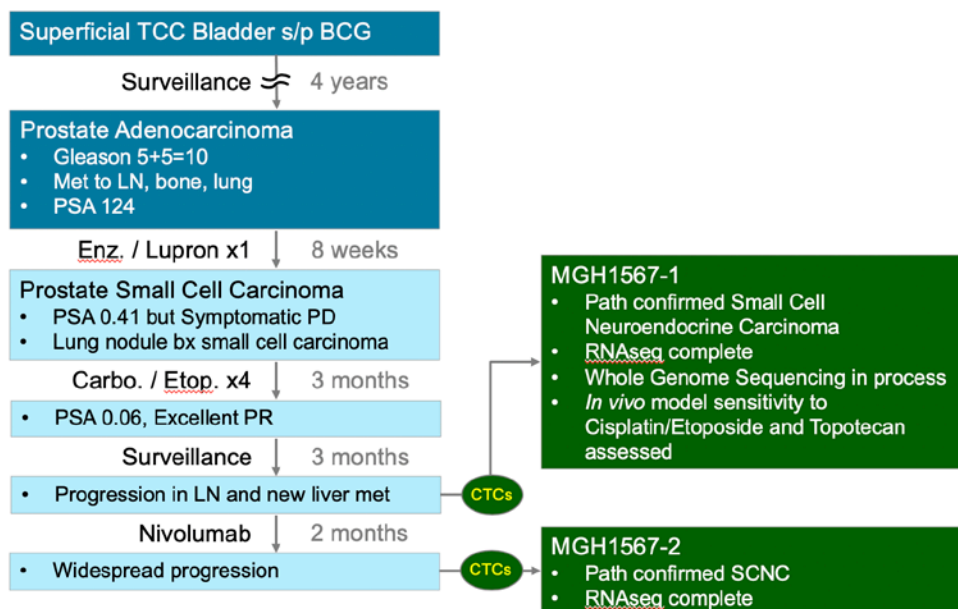
**Project Area 2:** We have successfully synthesized SMDC conjugates, overcoming technical barriers towards conjugate synthesis (see attached submitted manuscript by Guan et al, titled Chemically Identical Pair of Small-Molecule Theranostic Conjugates Specific for Prostate Cancer Imaging and Therapy)

**Project 3: Developing models of NEPC for testing:** The paucity of adequate models of NEPC has forced us to develop alternate models of NEPC. We have worked with Dr. Benjamin Drapkin at UTSW to build new models of NEPC. Ben has collected CTCs from patients with SCLCs and NEPCs and has implanted these tumors into NSG mice and created circulating tumor cell derived xenografts. These CDXs are more likely to be representative of the metastatic NEPC cell.



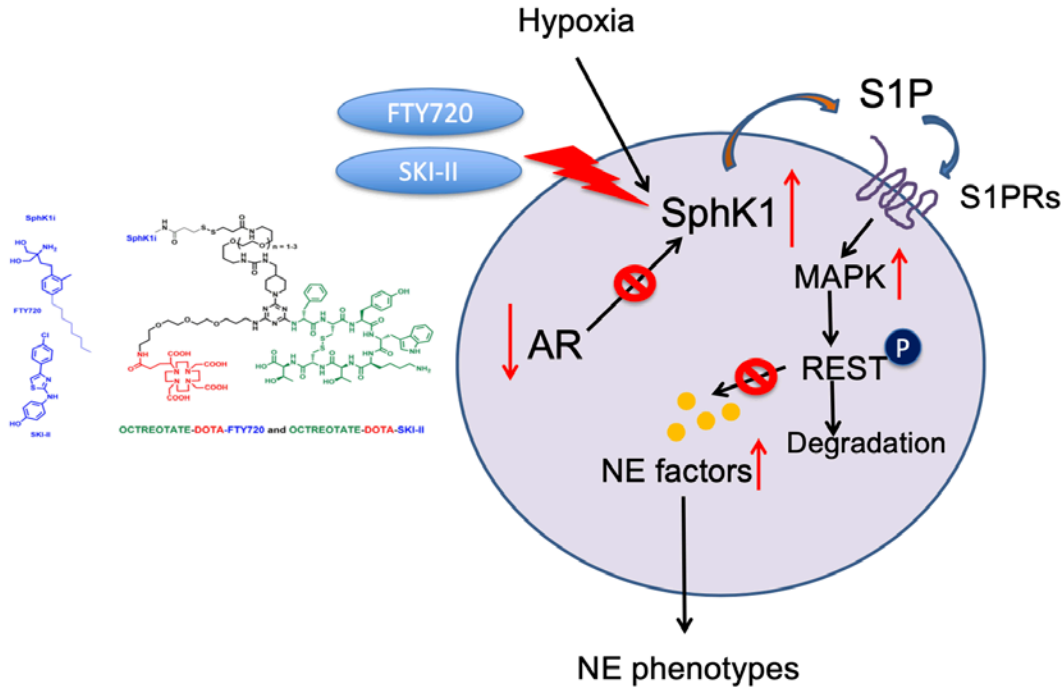
In collaboration with Daniel Haber and Shyamala Maheswaran

**We have derived 2 novel models of NEPC from one patient with NEPC and are further characterizing these models.** From RNA-seq evaluation, these are ASCL1-high models with classic small cell histology and compare favorably with the panel of small cell models



## Ongoing and Future work

1. Our goals are to further target SphK1 in NEPC and validate them in vivo models



2. For the synthetic pathway, we are setting up coupling reaction with the SKII linker, the key synthetic procedure for the construction of proposed conjugates.
3. We will further develop CDX models of NEPC and evaluate the effect of our SMDCs in vivo.



In terms of Specific Aims and SOW

Specific Aim 1	SOW Timeline	Status	Site
<b>Major Task:</b> Design, synthesize and evaluate the quality and biological activity of SMDCs	Months		
<b>Subtask 1:</b> To synthesize SMDCs	1-18		R/S
- Develop Hapten-DOTA-DM1 SMDC	1-6	Completed	S
- Design Hapten-DOTA-Sphk1 SMDC	4-9	Completed	S
- Develop Hapten-DOTA-Spk1 SMDC	10-18	Completed	S
- Develop <sup>68</sup> Ga <sup>177</sup> Lu-labeled SMDC	6-32	Ongoing	S
<b>Subtask 2:</b> To evaluate stability/ kinetics and cell uptake of SMDC/ bsMabs targeting Sphk1	1-34		
- Define kinetics of bsMab uptake by NEPC cells	1-18	Ongoing, on schedule	S
- In vitro stability of <sup>68</sup> Ga <sup>177</sup> -labeled SMDC	4-15	Ongoing	S,R
- Establish cell uptake of SMDCs	9-16	Ongoing	S,R
- Cell internalization assays	9-24	To be started	S,R
<b>Subtask 3:</b> To evaluate specificity of SMDC and bsMabs for NEPC and their molecular target- Sphk1	1-24		
- Generation of stable NEPC cells with CRISPR knockdown of Sphk1	1-12	Ongoing, behind schedule	R
- Generation of stable CRPC cells overexpressing Sphk1	1-12	Ongoing, on schedule	R
- Evaluation of the effect of the SMDCs and bsMabs targeting Sphk1 on stable NEPC and CRPC cells	9-24	To be started	S,R
<b>Subtask 4:</b> Establish the cytotoxicity of SMDCs targeting Sphk1	4-26		
- Evaluation in cell lines	4-16	Completed	R
- IRB approval	1-3	Completed	R
- Patient derived explant evaluation	4-34	Ongoing, on schedule	R
- Patient derived biopsy evaluation	4-34	Ongoing, on schedule	R
- Patient derived organoid evaluation	4-34	Ongoing, on schedule	R
<b>Milestone(s) Achieved</b>			
- Synthesis of SMDC targeting Sphk1	18	Ongoing, on schedule	S,R
- Stability/ kinetics. Cell uptake of SMDCs	34	Ongoing, on schedule	S,R
- Specificity of SMDC and bsMabs for NEPC and their molecular target- Sphk1	24	Ongoing, on schedule	S,R
- Cytotoxicity of SMDCs	36	Ongoing, on schedule	S,R

- <i>Manuscripts</i>	36	Ongoing, on schedule	S,R
<b>Specific Aim 2</b>			
<b>Major Task:</b> To evaluate the optimal sequence, toxicity and preclinical activity of SMDCs and bsMabs			
<b>Subtask 1:</b> To establish the toxicity and biodistribution of SMDCs and bsMabs.	1-24		
- <i>IACUC approval</i>	1-6	Completed	R
- <i>Generation of labeled SMDCs</i>	7-24	Completed	S,R
- <i>Toxicity studies</i>	7-24	Ongoing, on schedule	S,R
- <i>Biodistribution studies</i>	9-24	Ongoing, on schedule	R
<b>Subtask 2:</b> To evaluate biological activity of SMDC and bsMAbs with single dose administration	12-27		
• - <i>IACUC approval</i>	12-15	Behind schedule	S,R
• - <i>Generation of labeled SMDCs</i>	12-20	Behind schedule	S,R
• - <i>PET imaging</i>	16-27	on schedule	S,R
• - <i>Evaluation of drug activity</i>	16-27	on schedule	S,R
<b>Subtask 3:</b> To evaluate biological activity of SMDC and bsMAbs with multiple administrations	18-34		
- <i>IACUC approval</i>	18-21	Behind schedule	S,R
- <i>Generation of labeled SMDCs</i>	18-28	Behind schedule	S,R
- <i>PET imaging</i>	22-32	on schedule	S,R
- <i>Evaluation of drug activity</i>	22-34	on schedule	S,R
- <i>PDeX experiments</i>	26-34	on schedule	S,R
<b>Milestone(s) Achieved</b>			
- <i>Toxicity and biodistribution of SMDCs and bsMabs.</i>	24	on schedule	S,R
- <i>Biological activity of SMDC and bsMAbs with single dose administration</i>	27	on schedule	S,R
- <i>Biological activity of SMDC and bsMAbs with multiple administrations</i>	34	on schedule	S,R
- <i>Manuscripts</i>	36	on schedule	S,R

## RESEARCH ARTICLE

# The central role of Sphingosine kinase 1 in the development of neuroendocrine prostate cancer (NEPC): A new targeted therapy of NEPC

Cheng-Fan Lee<sup>1,2</sup>  | Yu-An Chen<sup>1</sup> | Elizabeth Hernandez<sup>1</sup> | Rey-Chen Pong<sup>1</sup> |  
Shihong Ma<sup>1</sup> | Mia Hofstad<sup>1</sup> | Payal Kapur<sup>3</sup> | Haiyen Zhau<sup>4</sup> |  
Leland WK Chung<sup>4</sup> | Chih-Ho Lai<sup>5</sup> | Ho Lin<sup>6</sup> | Ming-Shyue Lee<sup>2</sup> |  
Ganesh V Raj<sup>1,7</sup> | Jer-Tsong Hsieh<sup>1</sup> 

<sup>1</sup> Department of Urology, University of Texas Southwestern Medical Center, Dallas, Texas, USA

<sup>2</sup> Department of Biochemistry and Molecular Biology, College of Medicine, National Taiwan University, Taipei, Taiwan

<sup>3</sup> Urology and Pathology, University of Texas Southwestern Medical Center, Dallas, Texas, USA

<sup>4</sup> Uro-Oncology Research, Department of Medicine, Cedars-Sinai Medical Center, Los Angeles, California, USA

<sup>5</sup> Department of Microbiology and Immunology, Graduate Institute of Biomedical Sciences, College of Medicine, Chang Gung University, Taoyuan, Taiwan

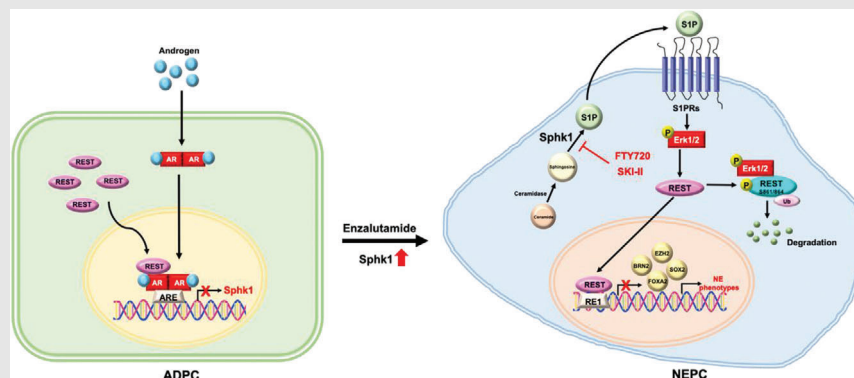
<sup>6</sup> Department of Life Sciences, National Chung Hsing University, Taichung, Taiwan

<sup>7</sup> Department of Pharmacology, University of Texas Southwestern Medical Center, Dallas, Texas, USA

## Correspondence

Jer-Tsong Hsieh, Department of Urology, UT Southwestern Medical Center, 5323 Harry Hines Blvd., Dallas, TX 75390, USA.  
Email: [jt.hsieh@utsouthwestern.edu](mailto:jt.hsieh@utsouthwestern.edu)


## Graphical Abstract



- Long-term hormonal therapy-elicited sphingosine kinase 1 (SphK1) gene transcription is modulated by androgen receptor (AR) and RE-1 silencing transcriptional factor (REST) repressor complex.
- SphK1 produces sphingosine-1-phosphate (S1P) to promote trans-differentiation of androgen-dependent prostate cancer (ADPC) into neuroendocrine prostate cancer (NEPC) in an autocrine manner.
- The binding of S1P to its receptors (S1PRs) activate Erk1/2 to phosphorylate REST at serine 861/864 sites leading to proteasomal degradation, which unleashes transcriptional repression of neuronal transcriptional factors expression.
- FDA approved SphK1-specific inhibitors (FTY720 or SKI-II) can overcome Enzalutamide-resistant CRPC tumor growth.

## RESEARCH ARTICLE

# The central role of Sphingosine kinase 1 in the development of neuroendocrine prostate cancer (NEPC): A new targeted therapy of NEPC

Cheng-Fan Lee<sup>1,2</sup>  | Yu-An Chen<sup>1</sup> | Elizabeth Hernandez<sup>1</sup> | Rey-Chen Pong<sup>1</sup> | Shihong Ma<sup>1</sup> | Mia Hofstad<sup>1</sup> | Payal Kapur<sup>3</sup> | Haiyen Zhau<sup>4</sup> | Leland WK Chung<sup>4</sup> | Chih-Ho Lai<sup>5</sup> | Ho Lin<sup>6</sup> | Ming-Shyue Lee<sup>2</sup> | Ganesh V Raj<sup>1,7</sup> | Jer-Tsong Hsieh<sup>1</sup> 

<sup>1</sup> Department of Urology, University of Texas Southwestern Medical Center, Dallas, Texas, USA

<sup>2</sup> Department of Biochemistry and Molecular Biology, College of Medicine, National Taiwan University, Taipei, Taiwan

<sup>3</sup> Urology and Pathology, University of Texas Southwestern Medical Center, Dallas, Texas, USA

<sup>4</sup> Uro-Oncology Research, Department of Medicine, Cedars-Sinai Medical Center, Los Angeles, California, USA

<sup>5</sup> Department of Microbiology and Immunology, Graduate Institute of Biomedical Sciences, College of Medicine, Chang Gung University, Taoyuan, Taiwan

<sup>6</sup> Department of Life Sciences, National Chung Hsing University, Taichung, Taiwan

<sup>7</sup> Department of Pharmacology, University of Texas Southwestern Medical Center, Dallas, Texas, USA

## Correspondence

Jer-Tsong Hsieh, Department of Urology, UT Southwestern Medical Center, 5323 Harry Hines Blvd., Dallas, TX 75390, USA.  
Email: [jt.hsieh@utsouthwestern.edu](mailto:jt.hsieh@utsouthwestern.edu)

Cheng-Fan Lee and Yu-An Chen contributed equally to this work.

## Funding information

Prostate Cancer Foundation, USA; The Ministry of Science and Technology in Taiwan, Grant/Award Numbers: MOST 108-2911-I-005-509, MOST 110-2926-I-005-502, MOST 104-2911-I-002-578, MOST 105-2911-I-002-521

## Abstract

**Background:** Neuroendocrine prostate cancer (NEPC) is often diagnosed as a sub-type from the castration-resistant prostate cancer (CRPC) recurred from the second generation of anti-androgen treatment and is a rapidly progressive fatal disease. The molecular mechanisms underlying the trans-differentiation from CRPC to NEPC are not fully characterized, which hampers the development of effective targeted therapy.

**Methods:** Bioinformatic analyses were conducted to determine the clinical correlation of sphingosine kinase 1 (SphK1) in CRPC progression. To investigate the transcriptional regulation SphK1 and neuroendocrine (NE) transcription factor genes, both chromosome immunoprecipitation and luciferase reporter gene assays were performed. To demonstrate the role of SphK1 in NEPC development, neurosphere assay was carried out along with several biomarkers determined by quantitative PCR and western blot. Furthermore, in vivo NEPC xenograft models and patient-derived xenograft (PDX) model were employed to determine the effect of SphK1 inhibitors and target validation.

This is an open access article under the terms of the [Creative Commons Attribution](https://creativecommons.org/licenses/by/4.0/) License, which permits use, distribution and reproduction in any medium, provided the original work is properly cited.

© 2022 The Authors. *Clinical and Translational Medicine* published by John Wiley & Sons Australia, Ltd on behalf of Shanghai Institute of Clinical Bioinformatics

**Results:** Significant prevalence of SphK1 in NEPC development is observed from clinical datasets. SphK1 is transcriptionally repressed by androgen receptor-RE1-silencing transcription factor (REST) complex. Furthermore, sphingosine 1-phosphate produced by SphK1 can modulate REST protein turnover via MAPK signaling pathway. Also, decreased REST protein levels enhance the expression of NE markers in CRPC, enabling the transition to NEPC. Finally, specific SphK1 inhibitors can effectively inhibit the growth of NEPC tumors and block the REST protein degradation in PDX.

**Conclusions:** SphK1 plays a central role in NEPC development, which offers a new target for this lethal cancer using clinically approved SphK1 inhibitors.

#### KEYWORDS

neuroendocrine prostate cancer, Sphingosine kinase 1, targeted therapy, therapy and castration resistant prostate cancer

## 1 | BACKGROUND

Prostate cancer (PCa) is an androgen-dependent disease and androgen deprivation therapy (ADT) is considered the most effective regimen to treat metastatic disease. However, almost all patients eventually develop castration-resistant PCa (CRPC) within 12 to 18 months of treatment with a median survival of 14 to 26 months, which is associated with the majority of mortality of this disease.<sup>1</sup> Although new agents, such as anti-androgen therapeutics (Enzalutamide or Abiraterone) or radiotherapy (Radium-223) or immunotherapy (Sipuleucel-T), have been introduced for these patients, CRPC inevitably acquires resistance known as therapy and castration-resistant PCa (t-CRPC).<sup>2,3</sup> Clinical observations<sup>4,5</sup> indicate that t-CRPC often exhibits distinct neuroendocrine (NE) phenotype with neuronal progenitor transcription factors (NETFs) expression and neuronal factors secretion in an endocrine fashion,<sup>6</sup> which is initiated by lineage plasticity of PCa leading to NE differentiation (NED) during CRPC progression.<sup>7</sup> Since NE PCa (NEPC) is resistant to ADT or radiotherapy,<sup>8,9</sup> unveiling the key molecular mechanism associated with NEPC progression could certainly lead to the development of new targeted therapeutics for NEPC.

The majority of PCa is adenocarcinoma (ADPC) that express androgen receptor (AR). In contrast, NEPC is characterized by a loss of AR expression, which attributes to ADT resistance. Also, the distinct expression of several NETFs (such as BRN2, EZH2, FOXA2 SOX2) and NE markers, such as chromogranin A (CgA) and synaptophysin (Syn), are associated with NEPC.<sup>10-13</sup> It is believed that

NEPC cells are trans-differentiated from ADPC. Recent studies unveil several intrinsic genetic drivers of NEPC such as loss of function of mutation in Rb and TP53 genes,<sup>13,14</sup> N-MYC amplification,<sup>15</sup> or overexpression of Aurora A kinase.<sup>16</sup> On the other hand, exogenous factors, including cytokines and growth factors,<sup>17</sup> are capable of inducing NE phenotypes in ADPC cell lines in vitro, suggesting an epigenetic regulation of NED.

The relationship between PCa development and lipid metabolism is well established.<sup>18</sup> Many studies showed an increase in total cholesterol and triglycerides levels upon treatment of ADT;<sup>19,20</sup> these changes support the notion that AR regulates lipid metabolism. Thus, it is believed that PCa patients receiving long-term (at least 12 months) ADT have a greater risk for metabolic syndrome compared with the men in the control groups.<sup>21,22</sup> However, the effect of lipid metabolism on NEPC progression is not well known. In this study, we report the promoting effect of sphingosine kinase 1 (SphK1) but not SphK2 on NEPC development, which could arise from either genetic alteration or transcriptional regulation mediated by the AR-RE1-silencing transcriptional factor (REST) complex. We have demonstrated that SphK1, catalyzes sphingosine to sphingosine-1 phosphate (S1P), which can promote NED of ADPC cells. Mechanistically, upon binding to its specific receptors, S1P can specifically activate the ERK signaling network, whose function is to accelerate the turnover of REST protein after phosphorylation leading to de-repression of many NETF genes transcription. Our findings reveal a new molecular mechanism by which NEPC development can be regulated by a lipid metabolite and further support Sphk1 as a potent therapeutic target for eradicating NEPC.

## 2 | MATERIALS AND METHODS

### 2.1 | Cell models, neurosphere assay and gene transfection

LNCaP, C4-2, C4-2B, 22RV1, NCI-H660 and PC3 were maintained in RPMI-1640 (Sigma-Aldrich) supplemented with 10% FBS (Gibco), 2 mM L-glutamine (Sigma-Aldrich), 1% Penicillin/Streptomycin (P/S) (Hyclone). VCAP cells were provided by Kenneth Pienta (Johns Hopkins University, Baltimore, MD, USA) and cultured in DMEM (Sigma-Aldrich) supplemented with 10% FBS, 2 mM L-glutamine and 1% P/S (Hyclone). IIB5 and IIG5 were single-cell clones derived from ARCaP<sup>23</sup> maintained in RPMI-1640 with 10% FBS, 2 mM L-glutamine and 1% v/v P/S. All cell lines were used within 10 passages and authenticated with the short tandem repeat (STR) profiling by Genomic Core in UT Southwestern Medical Center (UTSW) periodically. Mycoplasma testing was performed by MycoAlert kit (Lonza Walkersville) every quarter to ensure cells remained mycoplasma free.

Neurosphere assay<sup>24</sup> was carried out by plating cells (200–300 cells) in ultra-low plate containing Neurobasal medium (ThermoFisher Scientific), B27 Plus Supplement (ThermoFisher Scientific), 20 ng/mL basic fibroblast growth factor-2 (ThermoFisher Scientific) and 20 ng/mL epidermal growth factor (ThermoFisher Scientific) for 10 days. The number of sphere (larger than 50  $\mu\text{m}$  in diameter) imaged by microscope was counted to determine sphere-forming ability.

For gene transfection, cells ( $2.5 \times 10^5$ ) were seeded in a 60-mm dish at 60–70% confluency then transfected with plasmid vectors containing cDNA, luciferase reporter gene promoter or small hairpin RNAs (shRNA) constructs obtained from the National RNAi Core Facility (Academia Sinica) using either Xfect (Clontech) or JetPEI (Q-Bio Gene) transfection kit according to manufacturers' protocol.

### 2.2 | CRISPR/Cas9 gene knockout, small hairpin RNA knockdown and lentiviral particle preparation

Based on Feng Zhang's CRISPR guide design tool (<http://crispr.mit.edu/>), the guide RNAs for SphK1 gene knockout were designed: Ex2 or Ex3 (Supporting information Table S1) and subsequently cloned into lentiCRISPRv2 (Addgene). Small hairpin RNAs (shAR [TRCN0000314657]) for AR knockdown were obtained from the National RNAi Core Facility of Academia (Sinica, Taiwan). The PLKO vector was used as control.

For lentiviral particle preparation, Lenti-X 293T cell line (TakaRa) was used for transfection according to the manufacturer's protocol. Cells were cultured with OPTI-MEM serum-free media and transfected with the mixture of lentiviral package plasmids (pCMV- $\Delta\text{R8.91}$  and pMD.G) then viral suspension was harvested 24 h afterwards. The supernatant was then filtrated through a 0.45  $\mu\text{m}$  Steri-Flip filter (Millipore) and used for cell infection.

### 2.3 | Site-directed mutagenesis

The WT SphK1 tagged with FLAG at the carboxyl terminal was provided by Dr. Bink Wattenberg (James Graham Brown Cancer Center, KY, USA). The plasmid was used as the template to generate two SphK1 mutants (CA S225E and DN S225A) using site-directed mutagenesis kit (Agilent); the oligonucleotides were used for SphK1 CA S225E or DN S225A (Supporting information Table S1).

### 2.4 | Chromatin immunoprecipitation (ChIP), ChIP- reChIP and ChIP sequencing (ChIP-seq)

ChIP assay was performed by using ChIP-IT Express Enzymatic kit (Active Motif) according to the manufacturer's instructions. Briefly, cells were cross-linked with 1% formaldehyde for 10 min, quenched with glycine followed by nuclear lysis. After isolating nuclear fractions, chromatin was enzymatically sheared into 200–100 bp. The sheared DNA was immunoprecipitated with ChIP-grade antibodies for 16 h. After reversal of cross-linking, DNA fragments were purified on spin columns (Active Motif) subjected to DNA-seq. AR ChIP-REST reChIP was performed by using Magna ChIP A/G kit (Millipore) according to the manufacturer's instructions. Briefly, after treatment, cells were cross-linked with 1% formaldehyde for 10 min at room temperature and quenched with glycine followed by nuclear lysis. After isolating nuclear fractions, chromatin was sonicated and sheared into 200–100 bp with condition of amplitude: 30%, 15 s ON, 30 s OFF for 10 cycles. The sheared DNA was incubated with Magna-conjugated AR (Cell Signaling) antibody for 16 h and then separated into two portions. One portion of precipitated complex, after reversal of cross-linking, DNA fragments were purified on spin columns (Millipore) subjected to real-time PCR. For REST reChIP, AR ChIP complex was washed with stripping buffer for 1 h and incubated with Magna-conjugated REST antibody (Abclonal) for 16 h then samples were immunoprecipitated with Magna-conjugated

bead. After reversal of cross-linking, purified DNA fragments with spin columns (Millipore) were followed by real-time PCR. The data were normalized to IgG group. The primers used in this study are listed in Supporting information Table S1 and all the antibodies used in this study are listed in Supporting information Table S2.

## 2.5 | Gene promoter construction and luciferase reporter assay

Cells ( $2 \times 10^5$  per well) stably transfected with luciferase reporter plasmids were plated in six-well plate and were transfected with REST S861/864A plasmid using Xfect (Clontech) for 16 h. Next day, all cells were serum starved for 2 h before S1P ( $2.5 \mu\text{M}$ ) treatment for 4 h then subjected to luciferase reporter assay (Promega) determined by Monolight TD 20/20 luminometer (Turner Designs). The relative reporter gene activity was normalized with protein concentration. All transfection experiments were performed in triplicates.

## 2.6 | RNA isolation and quantitative real-time RT-PCR (qRT-PCR)

Total cellular RNA was extracted using Maxwell 16 LEV SimplyRNA Purification Kit (Promega) and  $2 \mu\text{g}$  RNA was reversely transcribed into cDNA using iScript cDNA Synthesis Kit (Bio-Rad). Real-time PCR analysis was set up with SsoAdvanced Universal SYBR Green Supermix Kit (BioRad) and carried out in MyiQ thermal cycler (Bio-Rad). All quantitative data of mRNA expression level were analyzed using  $\Delta C_t$  ( $C_t$  value normalized to 18S RNA) and  $\Delta\Delta C_t$  (difference between the  $\Delta C_t$  of control and experimental groups) values to obtain the fold change after normalizing with control group. The primers used in this study are listed in Supporting information Table S1.

## 2.7 | Western blot analyses and immunoprecipitation (IP)

Cells were lysed in ice-cold lysis buffer [150 mmol/L NaCl, 1% Triton X-100, 0.5% sodium deoxycholate, 0.1% SDS, 50 mmol/L Tri (pH 8.0), protease inhibitor cocktail (Roche)] and cell debris were removed by centrifugation at  $4^\circ\text{C}$  for 10 min at 12,000 rpm. Equal amount of protein was subjected to electrophoresis on NuPAGE gels (Life Technologies) then transferred onto nitrocellulose membranes. Subsequently, membranes were blocked with 2% non-fat dry milk w/v for 1 h and then incubated with primary antibodies (Supporting information Table S2). Appropri-

ate secondary antibodies conjugated with horseradish peroxidase and enhanced chemiluminescence were used to detect target proteins. Results were visualized with ECL chemiluminescent detection system (Pierce ThermoScientific). For immunoprecipitation (IP), AR antibody was pre-incubated with protein G Magna bead (Cell Signaling) for 1 h then  $300 \mu\text{g}$  protein lysate was incubated with Magna-conjugated AR for 16 h at  $4^\circ\text{C}$  and spun down. After washing three times, immunocomplex was eluted with buffer containing  $\beta$ -mercaptoethanol then heat denatured before SDS-PAGE. The relative protein expression level in each sample was normalized to actin.

## 2.8 | Determination of S1P production

Cells ( $1 \times 10^4$  cells per well) were seeded in 96-well plate with regular culture medium overnight then replaced by  $200 \mu\text{L}$  serum-free RPMI medium for 24 h. The supernatant was collected after centrifugation and subjected to ELISA kit (MyBioSource, MBS069092) for determining S1P production. For the patient-derived tumor explant (PDE) samples,  $10 \mu\text{g}$  of the homogenized tissue samples were subjected to ELISA. Three independent experiments were performed for statistical calculation and presented as mean  $\pm$  SD.

## 2.9 | In vitro cytotoxicity assay

Cells (5000 cells/well) were seeded onto the 96-well plate. After 24 h, fresh media containing different concentrations of FTY720 (Selleckchem), SKI-II (Selleckchem) or Opaganib (Selleckchem) were incubated for 48 h. In vitro cytotoxicity was measured using MTT (3-(4,5-Dimethylthiazol-2-yl) -2,5-Diphenyltetrazolium Bromide, Sigma-Aldrich) assay according to the manufacturer's instructions. The relative number of viable cells was determined using a microtiter plate reader at  $\text{OD}_{570 \text{ nm}}$ . The experiment was repeated in triplicate and data were represented as mean  $\pm$  SD.

## 2.10 | Tissue microarray and immunohistochemistry (IHC)

Formalin-fixed, paraffin-embedded sections were deparaffinized, rehydrated and subjected to heat-induced antigens retrieval (citrate buffer, pH 6.0) then incubated with appropriate primary antibody (Supporting information Table S2) and developed with 3, 3'-diaminobenzidine chromogen followed by counterstaining with hematoxylin and eosin. The H-score of immunohistochemistry (IHC)

was calculated by percentage of cytosolic staining (0: 0–5%; 1: 5–25%; 2: 25–75%; 3: 75–100%) × staining intensity (0: no staining; 1: weak staining; 2: moderate staining; 3: strong staining).

## 2.11 | Tumor xenografts

Three different NEPC ( $1 \times 10^6$  cells/site) cells were injected subcutaneously into the flank of castrated male NOD-SCID (6–8 weeks) mice. Once tumors became palpable, intraperitoneal injection of vehicle DMSO, FTY720 (15 mg/kg), SKI-II (15 mg/kg) or Enzalutamide (20 mg/kg) was injected three times per week for 2 weeks, then tumor volume was determined by caliper and calculated (length × width × width/2). All animal work was approved by the Institutional Animal Care and Use Committee.

## 2.12 | Patient-derived tumor explants (PDEs)

The ex vivo explant culture was performed as previously described.<sup>25</sup> Briefly, fresh PCa tissues were dissected into 1 mm<sup>3</sup> cube and placed on a Gelatin sponge (Novartis) bathed in RPMI-1640 media supplemented with 10% FBS, 100 units/mL P/S, 0.01 mg/mL hydrocortisone and 0.01 mg/mL insulin (Sigma-Aldrich). Tissues were treated with FTY720 or SKI-II (30 μM) for 48 h then were subjected to western blot analyses. The Institutional Review Board of UTSW approved the tissue procurement protocol for this study and written informed consent was obtained from all patients.

## 2.13 | Bioinformatics and statistical analyses

RNA-seq data were statistically analyzed based on the TCGA and CRPC database.<sup>26</sup> PCa patient survival rates were analyzed based on NCBI's Gene Expression Omnibus (GEO). The Prism Statistics (GraphPad) was used for all statistical analysis. Statistical significance,  $p < .05$  (\*) and  $p < .01$  (\*\*), was analyzed by Student's *t*-test. Data (mean ± SD) represented at least three independent experiments.

## 3 | RESULTS

### 3.1 | SphK1 is associated with NEPC development and confers Enzalutamide resistance of ADPC

Although PCa is a well-characterized lipid-rich tumor, the role of lipid metabolism or metabolite in PCa progression

is not fully characterized. SphK, with two isoforms (SphK1 and SphK2), is a bioactive enzyme capable of converting sphingosine into S1P, which is a lipid mediator playing a major regulatory role in tumor cell growth, survival, invasion, angiogenesis and therapeutic resistance.<sup>20–22</sup> Until now, the role of SphK in NEPC progression is largely unknown. It appears that SphK1 gene amplification is found in approximately 20% of NEPC and 16% of CRPC patients (Figure 1A). In contrast, Sphk2 gene amplification is not apparent in NEPC patients (Supporting information Figure S1A). RNA-seq data from NEPC/CRPC<sup>11,26</sup> and NEPC sub-lines derived from an androgen-deprived LNCaP model further support the correlation of SphK1 elevation with NEPC (Supporting information Figure S1B). A positive correlation between the mRNA expression of SphK1 and several NETFs (such as BRN2, FOXA2 and SOX2) as well as NE markers, CgA and Syp, can be found in PCa specimens derived from TCGA database (Figure 1B). Also, IHC data from PCa TMA indicated a positive correlation between SphK1 and Syp expression (Figure 1C). Furthermore, using PCa PDE model, S1P can induce BRN2, FOXA2 and Syp protein expression (Figure 1D and Supporting information Figure S1C). Additionally, a similar correlation from two well-characterized NEPC cell lines (such as PC3 and NCI-H660) but not from the ADPC cell line LNCaP is observed (Supporting information Figure S1D). Indeed, elevated SphK1 protein expression was detected in a variety of cell models (such as 22RV, ARCaP-IIB5 and -IIG5, and PC3) expressing NE phenotype compared with that in AR-positive ADPC cell models (such as LNCaP, C4-2, C4-2B and VCAP) (Supporting information Figure S1E), however, the ubiquitous expression of SphK2 was associated with every PCa cell lines. Overall, these data support a promoting role of SphK1 in NEPC development.

To demonstrate the impact of Sphk1 on NEPC progression with androgen-independent growth and Enzalutamide resistance, we performed constitutive active (CA) form of SphK1 with transformation at serine (S) 225 site into glutamic acid (E), which increases catalytic activity and induces translocation into the plasma membrane.<sup>27,28</sup> Then, LNCaP and ADPC cell lines were transfected with the constitutive active-SphK1 (S225E) that can increase the levels of extracellular S1P (Supporting information Figure S1F) and promote androgen-independent growth as well as the NED evidenced by the elevation of several NETFs and NE markers at both protein and mRNA levels (Figure 1E) as well as in vitro cell growth (Supporting information Figure S1F). Hence, we further investigated the role of SphK1 in developing Enzalutamide resistance of PCa by co-culturing both vector control (VC) LNCaP labeled with mCherry and CA-SphK1 LNCaP labeled with GFP at 100:1 ratio in the presence of Enzalutamide

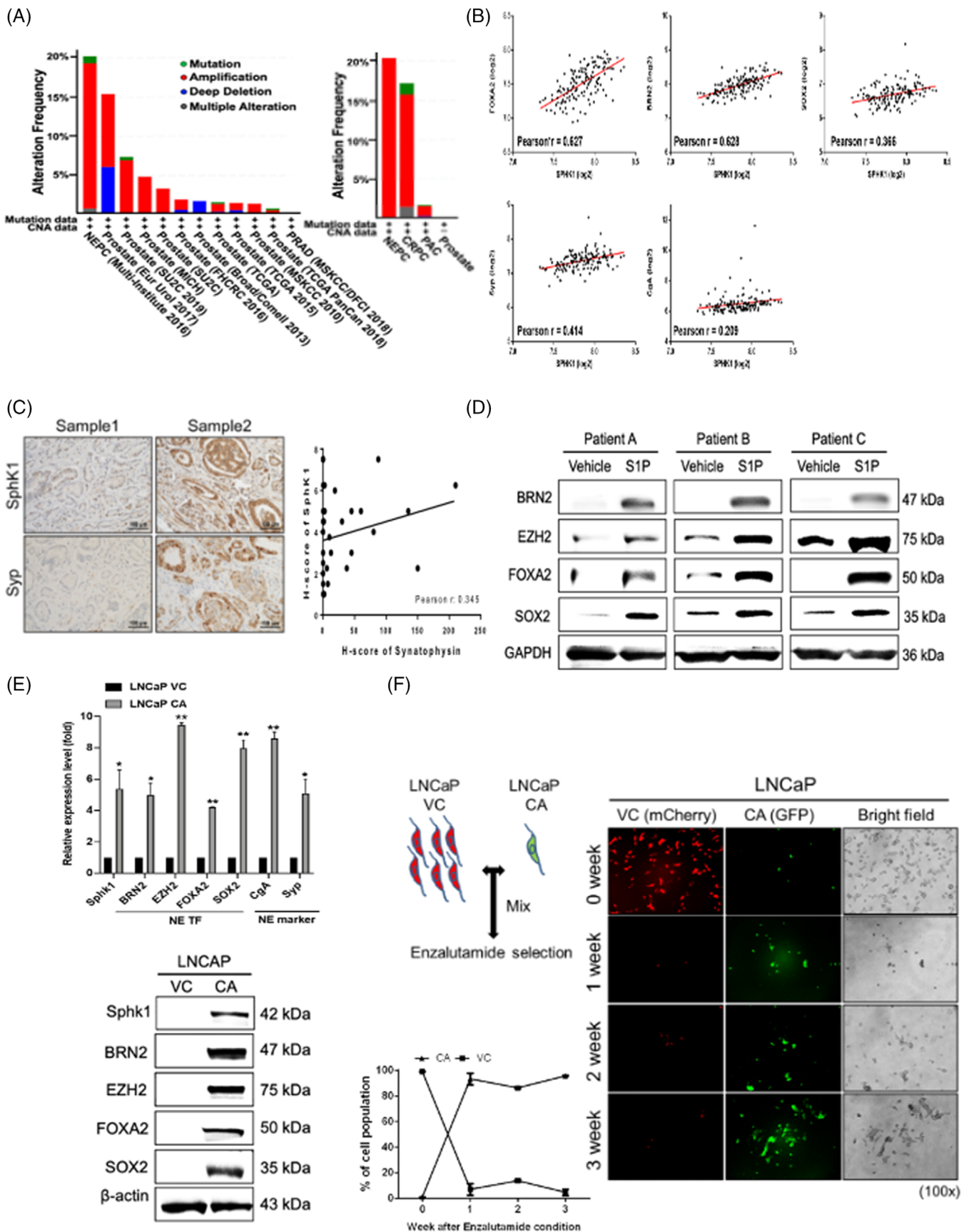


**FIGURE 1** The association of Sphk1 expression with NEPC progression. (A) The frequency of SphK1 gene alterations (green: mutation; blue: deletion; red: amplification) in PCa patients (cBioPortal database). (B) The positive correlation of mRNA expression between SphK1 and NE-related genes (BRN2, FOXA2, SOX2, CgA, Syp) in PCa patients (Betastasis Database). (C) The positive correlation of SphK1 and Syp

(Figure 1F, right panel). Long-term (3 weeks) androgen deprivation leads to a growth advantage of CA-SphK1 LNCaP cells. Thus, these data demonstrate that SphK1 activation is one of the key underlying mechanism of developing ADT resistance and contributes to NED in PCa cells.

### 3.2 | AR in co-operation with REST directs transcriptional repression of SphK1

Noticeably, there is an inverse correlation of AR and SphK1 protein expression in PCa (Supporting information Figures S1E and S2A), suggesting that a potential regulatory mechanism of both genes. Transcriptomic analyses of PCa databases indicated a similar negative correlation between SphK1 and AR or AR-regulated genes (such as ABCC4, APPBP2, TMPRSS2 and TDD52)<sup>29</sup> (Figure 2A and Supporting information Figure S2B). Also, GEO datasets of LNCaP cells treated with dihydrotestosterone (DHT) for 24 h (Figure 2B) or R1881 with a time course (3 to 48 h) (Figure 2C) clearly demonstrate the suppressive effect of androgen on SphK1 expression. Indeed, the inhibitory effect of DHT on SphK1 mRNA (Figure 2D) and protein (Supporting information Figure S2C) expression in LNCaP cells cultured in androgen deprived condition (i.e., phenol-red free and charcoal-stripped FBS) for 48 h; this inhibitory effect can be abolished in the presence of Enzalutamide (Figure 2D) or AR knock-down LNCaP cells (Left panel, Supporting information Figure S2D). This observation is further supported by the fact that Enzalutamide alone could increase SphK1 expression in LNCaP cells and Enzalutamide-resistant LNCaP (i.e., LNCAP MDVR) cells exhibited highly elevated SphK1 (Middle panel, Supporting information Figure S2D). Consistently, increased S1P production was observed in LNCaP treated with Enzalutamide for 24 h (Right panel, Figure S2D). It is known that constitutively active AR variant (ARV7) can bind to androgen response element (ARE) motif.<sup>30,31</sup> Thus, ARV7 overexpression in PC3 cells can suppress SphK1 expression (Supporting information Figure S2E). Moreover, DHT can inhibit SphK1 expression in PC3 cells-expressing AR (Supporting information Figure S2F). All these results indicate that SphK1 is an AR-repressed gene.

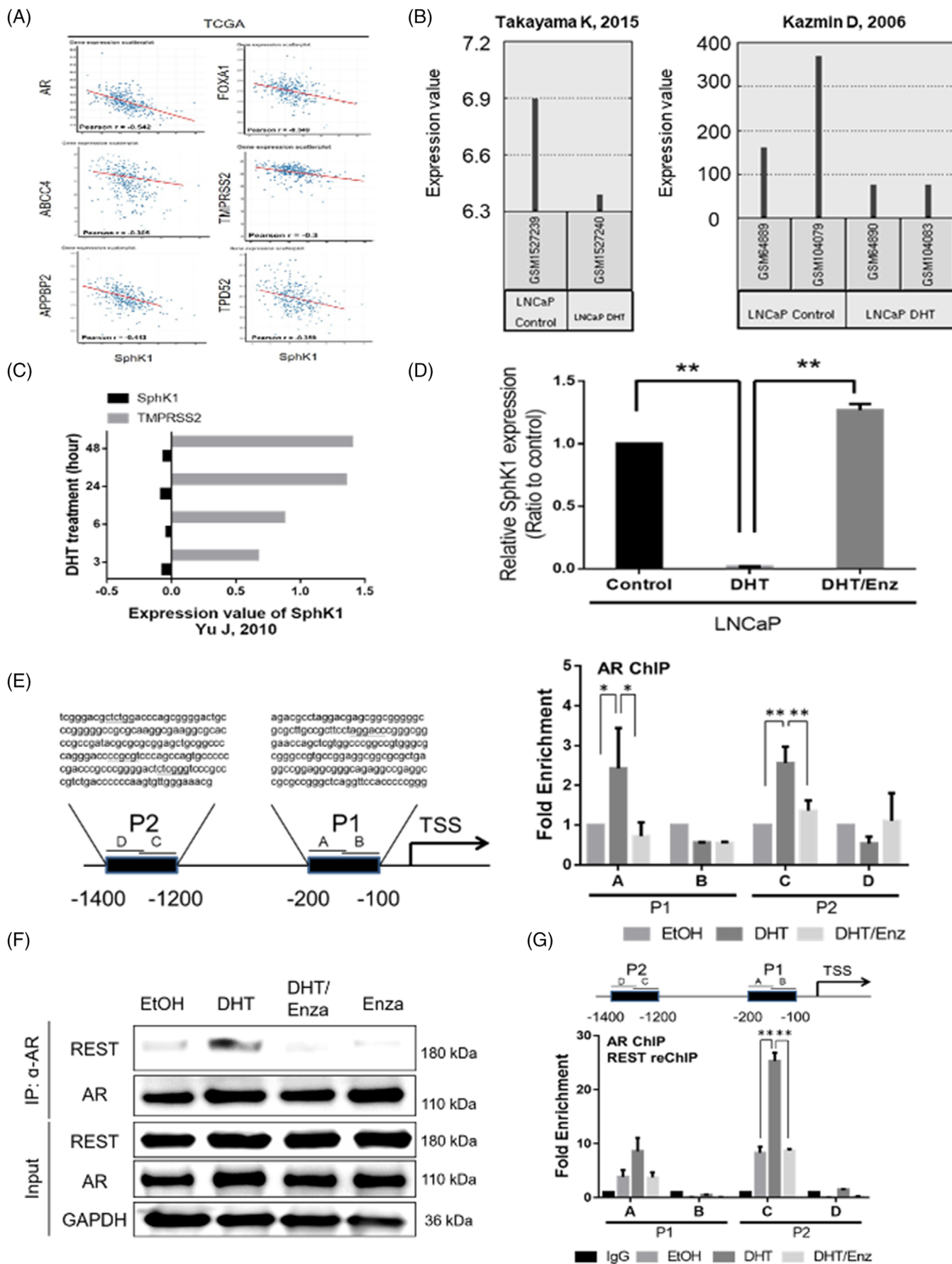
We further performed an AR motif search within the region upstream of the *SPHK1* gene and found four clusters of potential ARE at the region (-104 to -118, -1245 to -1259, -1284 to -1298 and -1373 to -1387) of the Sphk1 promoter. As shown in Figure 2E, two AR binding sites (A: -127 to -198 and C: -1215 to -1291) were confirmed by ChIP assay; DHT treatment increased the binding of AR to both sites, which was diminished by Enzalutamide (Figure 2E). Indeed, DHT (Figure 2F) can increase the complex formation between AR and REST known as an AR co-repressor.<sup>32</sup> In contrast, Enzalutamide can interrupt this complex formation (Figure 2F). As expected, AR ChIP-REST reChIP data support the binding of AR-REST complex to these two ARE sites (Figure 2G). These results support that the presence of REST is responsible for AR-suppressed SphK1 gene transcription.

### 3.3 | The enzymatic activity of Sphk1 is required for NED of PCa

To determine the role of SphK1 in the NED of PCa, the SphK1 gene was knocked out using two different sgRNA CRISPR constructs (i.e., EX2 and EX3) in several PCa cells-expressing NE phenotypes. These constructs exhibited specific SphK1 gene knockout without changing SphK2 levels (Top panel in Figure 3A to C), which is highly associated with decreased S1P production extracellularly (Supporting information Figure S3A). Loss of SphK1 is associated with the reduced expression of NETFs (BRN2, EZH2, FOXA2 and SOX2) and NE markers (CgA and Syp) at mRNA (Middle panel in Figure 3A to C and Left panel in Supporting information Figure S3B) and protein (Bottom panel in Figure 3A to C and Right panel in Supporting information Figure S3B) levels. It is known that NE feature can be acquired through neurosphere formation as neural stem cell activities. We demonstrated that SphK1 gene knockout or enzymatic inhibitors (such as FTY720 and SKI-II) could significantly decrease neurosphere formation in IIG5 (Figure 3D) and 22RV1 (Figure 3E) cells, indicating the driver role of SphK1 but not of Sphk2 in NED of PCa.

In Sphk1 gene knockout cells, exogenous S1P can induce NETFs (BRN2, EZH2, FOXA2 and SOX2) gene transcription in a dose-dependent manner, where as low as serum level of S1P (1  $\mu$ M) is sufficient to restore NETFs gene

expression using IHC on PCa TMA (n = 44). (D) Increased NETFs (BRN2 and FOXA2) and NE marker (Syp) protein expression in patient-derived explants treated with 100  $\mu$ M S1P for 24 h. (E) The induction of NETFs and NE markers in LNCaP cells expressing CA-SphK1. (F) The stimulatory effect of CA-SphK1 on the growth of LNCaP under androgen deprived condition (20  $\mu$ M Enzalutamide). Left top panel: Scheme of co-culture of VC cells (mCherry<sup>+</sup>) and CA-SphK1 cells (GFP<sup>+</sup>) at ratio 100:1 incubated with 20  $\mu$ M Enzalutamide for 3 weeks. Left bottom panel: Cell growth of two different LNCaP sub-lines treated with Enzalutamide. Right panel: Images of two different LNCaP sub-lines treated with Enzalutamide. \**p* < .05; \*\**p* < .01



expression (Supporting information Figure S3C). Similar induction of NETFs and NE markers (CgA and Syp) mRNA expression by exogenous S1P was observed in LNCaP cells (Supporting information Figure S3D). Moreover, in LNCaP MDVR with a high level of SphK1, SKI-II can decrease NETFs and NE markers mRNA (Left panel in Supporting information Figure S3E) and protein (Right panel in Supporting information Figure S3E) expression, which can be rescued by the addition of exogenous S1P. As expected, the presence of CA-SphK1 can significantly promote neurosphere formation in ADPC cells (LNCaP and C4-2) but SphK1 inhibitors can abolish the effect of CA-SphK1 (Supporting information Figure S3F). These results indicate that the enzymatic activity of SphK1 is required for the NED of PCa.

### 3.4 | SphK1-induced NED is mediated by S1P receptor (S1PR)-MAPK pathway

S1P action is mediated by specific S1P receptors (S1PRs), a class of G protein-coupled receptors that are associated with several downstream signaling pathways such as MAPK or PI3K-Akt or JAK-STAT.<sup>33</sup> To unveil the underlying signaling pathway, SphK1 knockout PCa cells were treated with exogenous S1P before the addition of specific inhibitors for MAPK (e.g., PD98059 or GSK1120212) or PI3K-Akt (e.g., LY294002 or BEZ235) or JAK inhibitor (e.g., Ruxolitinib) and the results (Figure 4A and B and Supporting information S4A-C) indicated the exclusive role of MAPK pathway in S1P-induced NED of PCa cells. In addition, S1PR1 inhibitor (Siponimod) can antagonize S1P-induced NED of PCa cells via MAPK pathway (Supporting information Figure S4D), supporting the mechanism of action of S1P is mediated through the binding of S1PRs. Altogether, these data clearly support the key role of MAPK pathway in the autocrine induction of NED in PCa cells by SphK1.

### 3.5 | MAPK-induced REST degradation underlies SphK1-induced NED

Knowing MAPK pathway can elicit a panel of NETFs gene expression, this action is likely mediated by a master

regulator. During neurogenesis, REST is characterized as a master transcriptional repressor in silencing neuronal gene expression and is degraded in neural progenitors to promote the subsequent elaboration of a mature neuronal phenotype.<sup>34</sup> In PCa, REST has been reported as the transcriptional inhibitor in IL-6-induced NED<sup>35</sup> and hypoxia-induced NED.<sup>36</sup> In SphK1 knockout PCa cells, accumulation of REST protein is evident (Figure 4C and Supporting information Figure S4E). In contrast, S1P can reduce REST protein levels that can be reversed in the presence of MAPK inhibitor (Right panel in Figure 4A and B), implying a role of the MAPK pathway in modulating REST. A previous study<sup>37</sup> demonstrated that S861/864 phosphorylation of REST facilitates the elimination of REST protein during the transition to neurons. By transfecting REST (S861/864A) construct, an unphosphorylated mutant, into several NEPC cells, a reduction of NETFs protein expression was observed (Figure 4D and Supporting information S4F). Despite elevated Erk phosphorylation in PC3 cells treated with S1P, the presence of REST (S861/864A) was able to suppress NETFs expression (Figure 4E). Also, in ADPC cells, such as C4-2 and LNCaP, CA-SphK1 (S225E) but not dominant-negative (DN)-SphK1 (S225A), can activate Erk leading to the reduction of REST, which leads to the elevation of NETFs expression (Supporting information Figure S4G). Taken together, the underlying mechanism of SphK1-induced NED is mediated via the activation of MAPK pathway that causes the degradation of serine phosphorylated REST by Erk.

### 3.6 | REST is master repressor of NETF gene transcription

To determine the role of REST in NETF gene transcription, REST ChIP-seq was performed to map the binding sites of REST on each NETF gene (Figure 5A). As shown in Figure 6B, SphK1 gene knockout can increase REST binding to each NETF gene promoter, which is similar to the expression of REST (S861/864A) in either PC3 or IIG5 cell (Figure 5B). In contrast, S1P treatment can significantly decrease REST binding to each NETF gene promoter (Figure 5B). By constructing luciferase reporter vectors from each gene promoter (Supporting information

**FIGURE 2** The suppressive effect of AR on Sphk1 gene expression. (A) An inverse correlation of mRNA expression between SphK1 and AR-regulated genes (AR, ABCC4, APPBP2, TMPRSS2 and TDD52) from TCGA database. (B) Decreased SphK1 gene expression in LNCaP cells treated with vehicle or DHT for 24 h (GSE62454, GSE436). (C) Time course effect of R1881 on the expression of SphK1 and TMPRSS2 genes in LNCaP cells (GSE14097). (D) The opposite effect of 10 nM DHT or 20  $\mu$ M Enzalutamide on SphK1 mRNA expression in LNCaP cells. (E) The impact of 10 nM DHT or 20  $\mu$ M Enzalutamide on the binding of AR for predict androgen recognition element (ARE, underline) in SphK1 promoter at P1 (A, B) and P2 (C, D) region. (F) The impact of 10 nM DHT or 20  $\mu$ M Enzalutamide on the interaction between AR and REST proteins. (G) The impact of 10 nM DHT or 20  $\mu$ M Enzalutamide on the binding of AR-REST complex to predict ARE in SphK1 promoter. \* $p < .05$ ; \*\* $p < .01$

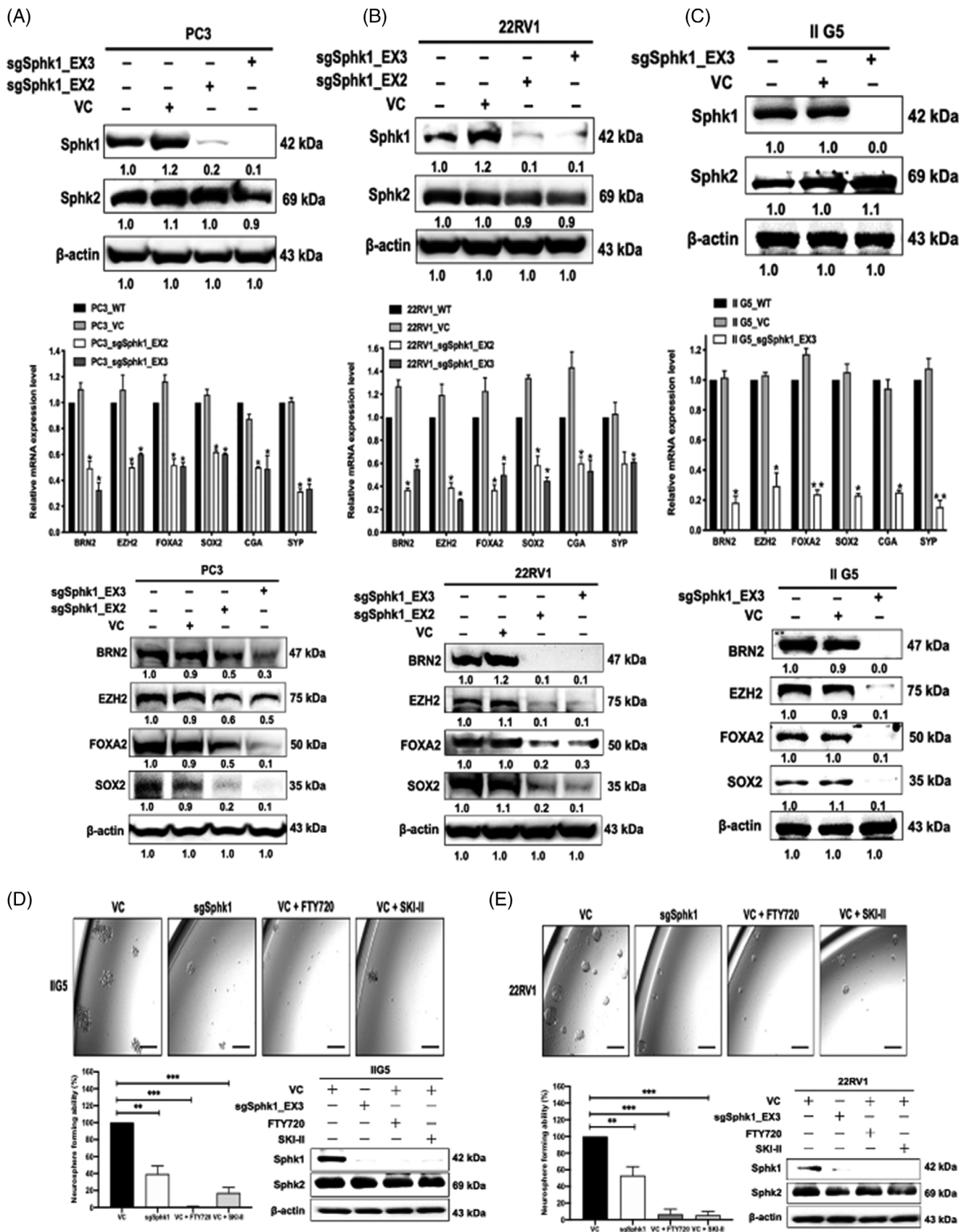


**FIGURE 3** The role of SphK1 in the onset of NEPC. (A, B, C) Top panel: Decreased SphK1 protein expression in several SphK1 knockout (sgSphK1) PCa cells. Middle panel: Decreased mRNA expression of BRN2, EZH2, FOXA2, CHA and SYP gene in sgSphK1 cells. Bottom panel: Decreased protein expression of BRN2, EZH2, FOXA2 and SOX2 protein level in sgSphK1 cells. (D, E) The effect of SphK1 on neurosphere formation of IIG5 or 22RV1 cells

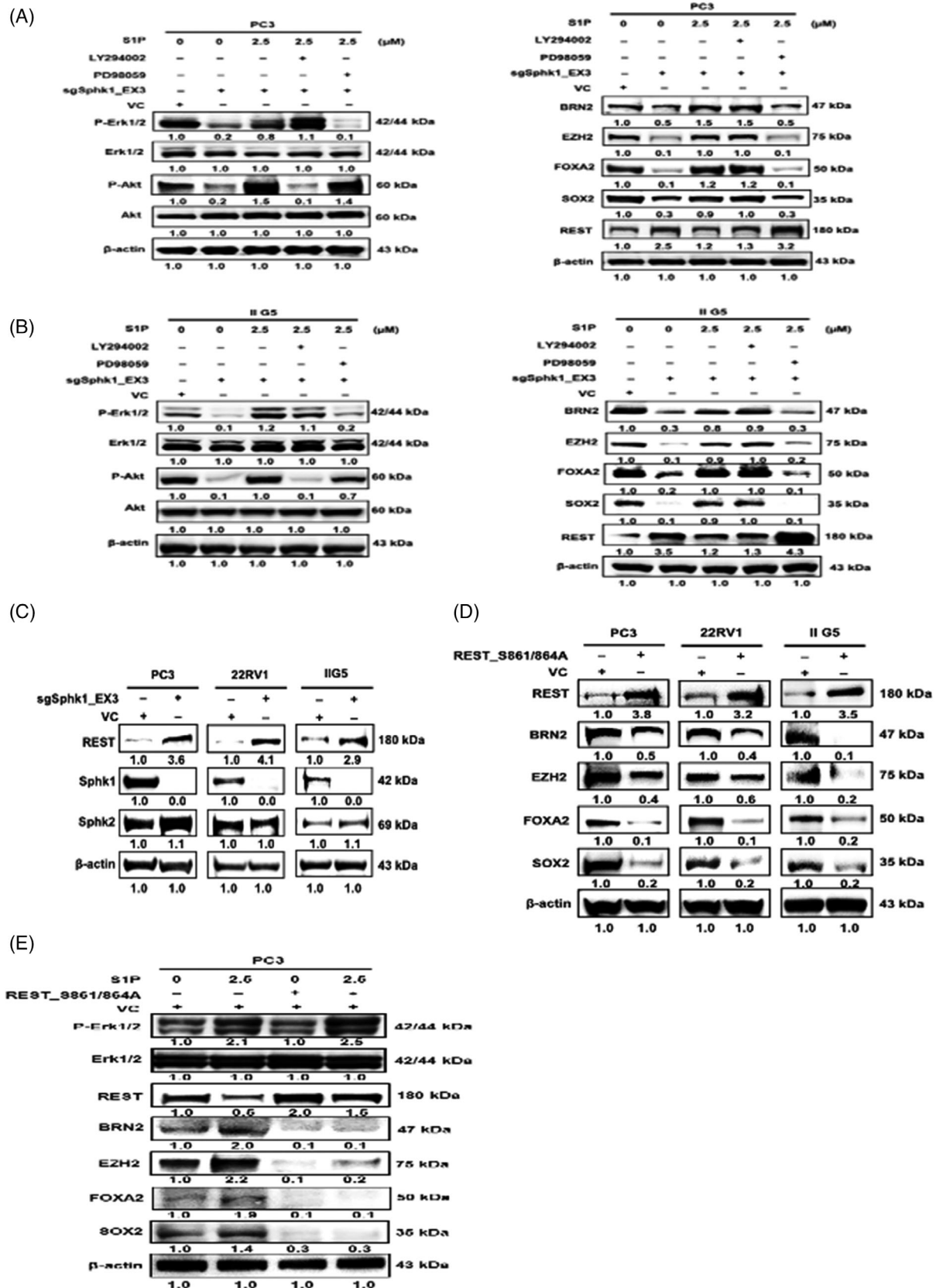
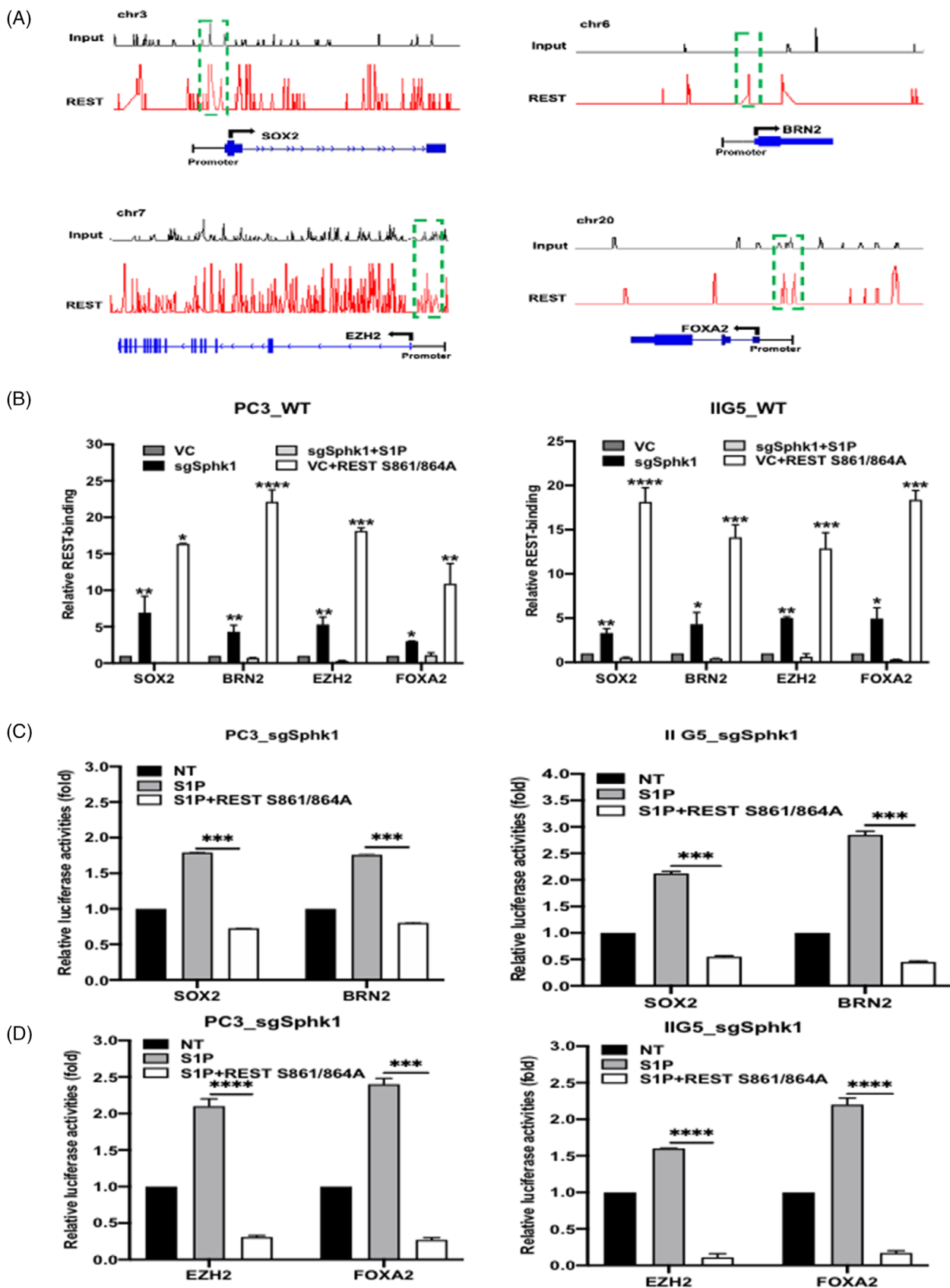
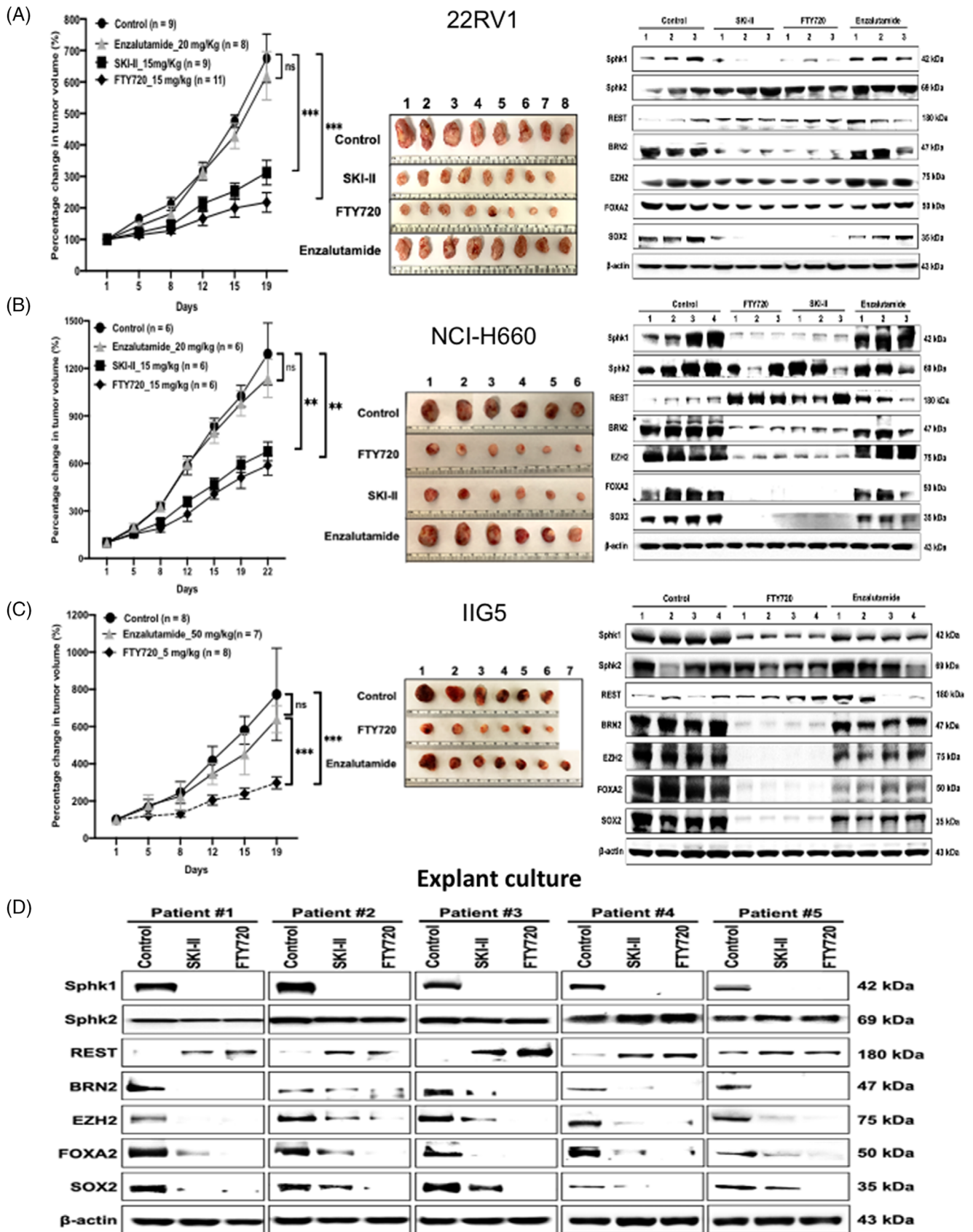


FIGURE 4 The S1P-elicited signaling pathway leading to the onset of NEPC. (A, B) Left panel: The specificity of PI3K inhibitor (LY294002) or MEK inhibitor (PD98059) on inhibiting the activation of respective kinase (Akt S473 phosphorylation or Erk phosphorylation). Right panel: The effect of LY294002 or PD98059 on S1P-induced NETF protein expression. (C) Accumulation of REST protein in SphK1 knockout- PC3, 22RV1 and IIG5 cells. (D) The effect of REST mutant (S861/864A) on NETF protein expression in PC3, 22RV1 and IIG5 cells. (E) The antagonistic effect of REST mutant (S861/864A) on S1P-elicited NETF expression in PC3 cells. \* $p < .05$ ; \*\* $p < .01$



**FIGURE 5** The suppressive role of REST in S1P-induced NETF genes transcription. (A) Annotation of REST binding sites in each NETF gene promoter. (B) ChIP-qPCR analyses of REST occupancy at promoter region of NETF genes in PC3 and IIG5 cells. (C, D) The effect of REST mutant (S861/864A) on S1P-induced SOX2, BRN2, EZH2 and FOXA2 promoter activity in SphK1 knockout—PC3 and IIG5 cells. \* $p < .05$ ; \*\* $p < .01$ ; \*\*\* $p < .001$ ; \*\*\*\* $p < .0001$



**FIGURE 6** The potency of SphK1 inhibitors on NEPC therapy. (A, B, C) Left and Middle panel: The in vivo potency of SphK1 inhibitors in Enzalutamide-resistant NEPC tumor models. Right panel: Target validation in tumor specimens harvested from the end of each treatment. (D) The inhibitory effect of SphK1 inhibitors on NETF protein expression in PDX models. \*\* $p < .01$ ; \*\*\* $p < .001$

Figure S5A), S1P treatment can induce the activities of each gene promoter, however, the presence of REST (S861/864A) can significantly inhibit these activities (Figure 5C and D and Supporting information Figure S5B-E). Taken together, these results support the master suppressive role of REST in NED of PCa.

### 3.7 | SphK1-specific inhibitors are potent therapeutics for NEPC tumor

As shown in Supporting information Figure S6A, the heterogeneous expression of S1PRs in each PCa cell line is noticed, suggesting that SphK1 is considered as a better druggable target. Thus, we first tested two small molecule inhibitors (SMIs) SKI-II and FTY720 with different mechanisms of action.<sup>33</sup> From a panel of 22RV1 cell models, we found that either WT or VC cell was highly sensitive to both inhibitors with IC<sub>50</sub> approximately 5  $\mu$ M (Supporting information Figure S6B). However, both SphK1 knockout cells were resistant to both inhibitors (Supporting information Figure S6A), supporting the specificity of both agents. Both inhibitors are able to reduce colony formation (Supporting information Figure S6C) and induce cell apoptosis (Supporting information Figure S6D). Also, the SphK2 inhibitor (Opaganib, ABC294640) failed to show any inhibitory effect on NEPC cells (Supporting information Figure S6E). Subsequently, we evaluated the therapeutic efficacy of SKI-II and FTY720 (Fingolimod) in comparison with Enzalutamide using three NEPC tumor models (i.e., IIG5, 22RV1 and NCI-H660). As expected, all three of these models are resistant to Enzalutamide (Figure 6A-C). In contrast, both SphK1 inhibitors exhibited a significant growth inhibition (Left and Middle panel in Figure 6A-C), which could be further validated by profiling the expression of drug target or NEPC-associated biomarkers (Right panel in Figure 6A-C). Noticeably, during the entire course of treatment, no significant toxicity was observed with both compounds (Supporting information Figure S6F-H). Furthermore, by employing PDE as a pre-clinical human model for drug target and surrogate biomarkers validation, both agents clearly reduced SphK1 and NETFs expression and exhibited target-specificity without altering SphK2 levels (Figure 6D). In those treated specimens, we also observed elevated REST (Figure 6D), supporting the mechanism of action of SphK1 in NEPC progression. Therefore, SKI-II and FTY720 are potent SphK1 SMIs with an immediate impact on clinical trial of NEPC therapy.

## 4 | DISCUSSION

Despite initial effectiveness, second-generation AR antagonists with higher anti-androgen activities facilitate the

progression of CRPC to less characterized NEPC with aggressive phenotypes. Until now, few therapeutic options are available due to a lack of druggable targets. Clinically, the majority of PCa is ADPC, and NEPC is rarely identified at the primary site. However, the appearance of NEPC from metastatic PCa after ADT<sup>38</sup> is believed to ADPC acquired lineage plasticity and trans-differentiation. Over the past 10 years, many efforts have been made to unveil the molecular mechanism of NEPC development. For example, the frequent mutations of TP53 and Rb1 or over-expression of oncogenes (such as NMYC or Aurora-Kinase A) are now recognized as genetic pre-disposition factors. However, the mechanism-based targeting strategy is still under-developed.

Based on clinical database or PCa cell models (Figure 1 and Supporting information Figure S1), SphK1 but not SphK2 is highly associated with NEPC development. Despite SphK1 and SphK2, which contribute to intracellular S1P level, but only SphK1 produces extracellular S1P (Figure 1D, Supporting information Figure S1C and F) leading to S1PR cascade in NE features. It appears that long-term ADT leading to lost or reduced AR expression becomes apparent in clinical NEPC, implying AR may be able to suppress NEPC development. ADT is also known to generate stress on tumor-surrounding milieu by increasing tissue hypoxia or production of many secretory factors, such as cytokines (IL-6, IL-8), known to induce NED of PCa,<sup>39</sup> in parallel with genetic alteration. Our data conclude that SphK1 plays an autocrine role in NEPC onset from CRPC (Figure 7A) and it is a bona fide AR-repressed gene in PCa cells, which is regulated by the AR-REST complex (Figure 2 and Supporting information Figure S2). REST is characterized not only as an AR co-repressor but also as a neuron-specific silencing factor (Figure 5) and master transcriptional repressor in neuronal cells, thus, it is often decreased in NEPC specimens.<sup>40</sup>

The long term of ADT is known to alter lipid metabolism,<sup>41,42</sup> our recent study<sup>43</sup> demonstrated that peroxisome proliferator-activated receptor  $\gamma$ , a major lipogenic transcription factor, is involved in IL-6-induced NED, indicating that the effect of lipid metabolism on NEPC development. SphK, categorized as a bioactive lipid enzyme, has two isoforms (SphK1 and SphK2) that play a central player in the sphingolipid rheostat. In mammals, SphK/S1P signaling is pivotal for normal physiology of neurogenesis, lymphocyte trafficking and vascular development through roles in cell proliferation, survival, differentiation, motility and intracellular calcium regulation.<sup>44,45</sup> SphK1 and SphK2 contributions to their diverse functions are due to differential expression of the number of each isozyme, conformation and dimerization properties and sub-cellular localizations. There is a strong

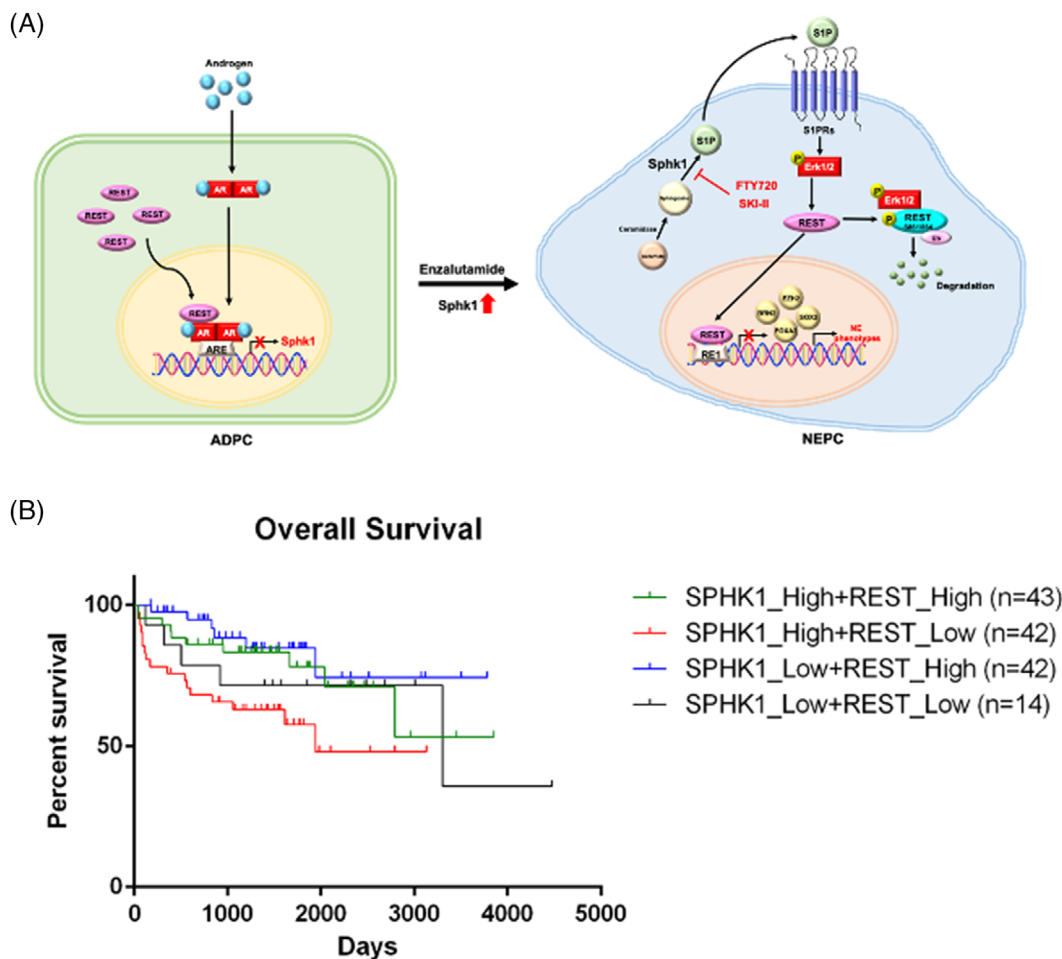


**FIGURE 7** The role of SphK1 in PCa progression. (A) The scheme of the reciprocal regulator network among SphK1, AR and REST in NEPC development. (B) Clinical correlation of SphK1 and REST with overall survival of PCa patients

suggestion that imbalances of SphK1 isoform abundance may play a crucial role in the pathophysiology of diverse diseases and may contribute to resistance to current anti-cancer drug therapies.<sup>46,47</sup> A wide range of S1P concentrations have been demonstrated its effect on cell proliferation or invasion from many solid tumor models<sup>48–59</sup> through binding to different S1PRs, G protein-coupled receptors.<sup>33</sup> In PCa, the role of SphK activities in cell proliferation is mediated through S1PR-activated PI3K/Akt pathway.<sup>60</sup> However, our data (Supporting information Figure S3C) from this study indicate that the serum level of S1P (~1  $\mu$ M) is sufficient to elicit NED via S1PRs (Supporting information Figure S4D). Mechanistically, our data indicate that S1P can activate MAPK pathway but not Akt or JAK-STAT pathway in PCa (Figure 4A and B and Supporting information Figure S4A–C) to increase REST phosphorylation at S861/864 sites leading to a rapid turnover by proteasome degradation (Figure 4C–E and Supporting information Figure S4E–F). Taken together, a reciprocal regulation between SphK1 and REST (Figure 7A) consistent with

clinical observations supports the significant correlation between PCa with  $Shpk1^{high}/REST^{low}$  with the poor overall survival (OS) of patients (Figure 7B); this pathway is independent from many genetic pre-disposition factors found in NEPC. Similarly, the expression of SphK1 is positively correlated with poor OS and progression-free survival (PFS) of breast cancer.<sup>61</sup> Also, a strong clinical evidence<sup>62</sup> indicates that lower REST expression is associated with aggressive breast cancers that most likely are estrogen receptor (ER) negative, implying the potential association of ER with REST. These parallel observations strengthen the critical role of SphK1 in PCa progression, which could prompt further investigation of the role of ER signaling in PCa progression via SphK1 activation.<sup>63</sup>

Our results (Figure 3D and E and Supporting information Figure S4D) indicate SphK1 or S1PRs as potential therapeutic targets. Although there are several available S1PR inhibitors, the heterogeneous expression of S1PRs in NEPC cells (data not shown) could hurdle drug selection. On the other hand, different classes of SphK1 SMIs

based on its substrate structure have been developed; many of them are under clinical trial for different diseases without significant side-effects. For example, FTY720 (Fingolimod), a S1P analog, is FDA-approved agent for treating multiple sclerosis. In this study, we first examined the effect of FTY720, and non-ATP-competitive SphK1 inhibitor, SKI-II in vitro and demonstrated that both specifically and potently targeted Sphk1 (Supporting information Figure S6A). In contrast, the SphK2 inhibitor failed to show any inhibitory effect (Supporting information Figure S6B). Furthermore, in vivo data indicated that three NEPC tumor models exhibiting Enzalutamide resistance responded both inhibitors (Figure 6A-C). During drug administration period, animals did not show significant toxicity based on total body weight (Supporting information Figure S6C). More importantly, we demonstrate that these inhibitors can specifically reduce the expression of SphK1 (but not SphK2) and NETF proteins (Figure 6A-C). Moreover, the drug target validation of both SphK1 inhibitors was confirmed using PDX model (Figure 6D). Our data conclude that repurposing of Sphk1 inhibitors could have an immediate impact on the development of NEPC targeted therapeutics. In addition, it is known that SphK1 conformation and activities can be influenced by several conditions including pH,<sup>64</sup> guanidinium chloride<sup>65</sup> and urea,<sup>66</sup> new SphK1 inhibitors have been developed for breast cancer treatment,<sup>67</sup> which could be applied for NEPC therapy in the future. Alternatively, SphK1 is found to interact with other kinases, such as CaMKII<sup>68,69</sup> that could provide additional targeting strategy for SphK1 activation in NEPC cells.

## 5 | CONCLUSIONS

The appearance of NE PCa in Enzalutamide- or Abiraterone-resistant CRPC patients represents lethal phenotype of PCa. Currently, there is no FDA-approved targeted therapeutics for NEPC. This study identified clinical prevalence of a bioactive lipid kinase, SphK1, in NEPC tumors and unveiled the signaling cascade in promoting the expression of many NE regulators and factors and neuronal stem cell activities. There is a unique reciprocal regulatory network among SphK1, AR and REST in modulating NED. Based on the central role of SphK1 in NEPC development, small molecule-specific inhibitors can overcome Enzalutamide resistance as well as tumor growth of several clinically relevant NEPC models and decrease NE biomarkers in PDE. Thus, repurposing FDA-approved SphK1 inhibitor has an immediate translational applicability to improve the outcome of NEPC patients to prolong their OS.

## ACKNOWLEDGEMENT

We would like to thank Mary Barnes for editorial assistance. This work was supported by a Grant from Prostate Cancer Foundation and the Ministry of Science and Technology in Taiwan (MOST 108-2911-I-005-509 and MOST 110-2926-I-005-502 to Ho Lin and Chih-Ho Lai, MOST 104-2911-I-002-578 and MOST 105-2911-I-002-521 to Ming-Shyue Lee).

## CONFLICT OF INTEREST

The authors declare that they have no conflict of interest.

## ORCID

Cheng-Fan Lee  <https://orcid.org/0000-0002-5043-2560>

Jer-Tsong Hsieh  <https://orcid.org/0000-0002-1919-6010>

## REFERENCES

- Gravis G. Systemic treatment for metastatic prostate cancer. *Asian J Urol.* 2019;6(2):162-168.
- Virgo KS, Basch E, Loblaw DA, et al. Second-line hormonal therapy for men with chemotherapy-naive, castration-resistant prostate cancer: American Society of Clinical Oncology Provisional Clinical Opinion. *J Clin Oncol.* 2017;35(17):1952-1964.
- Ritch CR, Cookson MS. Advances in the management of castration resistant prostate cancer. *BMJ.* 2016;355:i4405.
- Conteduca V, Aieta M, Amadori D, De Giorgi U. Neuroendocrine differentiation in prostate cancer: current and emerging therapy strategies. *Crit Rev Oncol Hematol.* 2014;92(1):11-24.
- Santoni M, Conti A, Burattini L, et al. Neuroendocrine differentiation in prostate cancer: novel morphological insights and future therapeutic perspectives. *Biochim Biophys Acta.* 2014;1846(2):630-637.
- Parimi V, Goyal R, Poropatich K, Yang XJ. Neuroendocrine differentiation of prostate cancer: a review. *Am J Clin Exp Urol.* 2014;2(4):273-285.
- Rubin MA, Bristow RG, Thienger PD, Dive C, Imielinski M. Impact of lineage plasticity to and from a neuroendocrine phenotype on progression and response in prostate and lung cancers. *Mol Cell.* 2020;80(4):562-577.
- Li Y, Chen HQ, Chen MF, et al. Neuroendocrine differentiation is involved in chemoresistance induced by EGF in prostate cancer cells. *Life Sci.* 2009;84(25-26):882-887.
- Hu CD, Choo R, Huang J. Neuroendocrine differentiation in prostate cancer: a mechanism of radioresistance and treatment failure. *Front Oncol.* 2015;5:90.
- Huang YH, Zhang YQ, Huang JT. Neuroendocrine cells of prostate cancer: biologic functions and molecular mechanisms. *Asian J Androl.* 2019;21(3):291-295.
- Bishop JL, Thaper D, Vahid S, et al. The master neural transcription factor BRN2 is an androgen receptor-suppressed driver of neuroendocrine differentiation in prostate cancer. *Cancer Discov.* 2017;7(1):54-71.
- Qi J, Nakayama K, Cardiff RD, et al. Siah2-dependent concerted activity of HIF and FoxA2 regulates formation of neuroendocrine phenotype and neuroendocrine prostate tumors. *Cancer Cell.* 2010;18(1):23-38.

13. Mu P, Zhang Z, Benelli M, et al. SOX2 promotes lineage plasticity and antiandrogen resistance in TP53- and RB1-deficient prostate cancer. *Science*. 2017;355(6320):84-88.
14. Ku SY, Rosario S, Wang Y, et al. Rb1 and Trp53 cooperate to suppress prostate cancer lineage plasticity, metastasis, and antiandrogen resistance. *Science*. 2017;355(6320):78-83.
15. Dardenne E, Beltran H, Benelli M, et al. N-Myc induces an EZH2-mediated transcriptional program driving neuroendocrine prostate cancer. *Cancer Cell*. 2016;30(4):563-577.
16. Li Z, Sun Y, Chen X, et al. p53 Mutation directs AURKA overexpression via miR-25 and FBXW7 in prostatic small cell neuroendocrine carcinoma. *Mol Cancer Res*. 2015;13(3):584-591.
17. Grigore AD, Ben-Jacob E, Farach-Carson MC. Prostate cancer and neuroendocrine differentiation: more neuronal, less endocrine? *Front Oncol*. 2015;5:37.
18. Galbraith L, Leung HY, Ahmad I. Lipid pathway deregulation in advanced prostate cancer. *Pharmacol Res*. 2018;131:177-184.
19. Mitsuzuka K, Arai Y. Metabolic changes in patients with prostate cancer during androgen deprivation therapy. *Int J Urol*. 2018;25(1):45-53.
20. Smith MR. Changes in fat and lean body mass during androgen-deprivation therapy for prostate cancer. *Urology*. 2004;63(4):742-745.
21. Torimoto K, Samma S, Kagebayashi Y, et al. The effects of androgen deprivation therapy on lipid metabolism and body composition in Japanese patients with prostate cancer. *Jpn J Clin Oncol*. 2011;41(4):577-581.
22. Nishiyama T, Ishizaki F, Anraku T, Shimura H, Takahashi K. The influence of androgen deprivation therapy on metabolism in patients with prostate cancer. *J Clin Endocrinol Metab*. 2005;90(2):657-660.
23. Zhau HY, Chang SM, Chen BQ, et al. Androgen-repressed phenotype in human prostate cancer. *Proc Natl Acad Sci USA*. 1996;93(26):15152-15157.
24. Palumbo P, Miconi G, Cinque B, et al. NOS2 expression in glioma cell lines and glioma primary cell cultures: correlation with neurosphere generation and SOX-2 expression. *Oncotarget*. 2017;8(15):25582-25598.
25. Ravindranathan P, Lee TK, Yang L, et al. Peptidomimetic targeting of critical androgen receptor-coregulator interactions in prostate cancer. *Nat Commun*. 2013;4:1923.
26. Beltran H, Prandi D, Mosquera JM, et al. Divergent clonal evolution of castration-resistant neuroendocrine prostate cancer. *Nat Med*. 2016;22(3):298-305.
27. Pitson SM, Xia P, Leclercq TM, et al. Phosphorylation-dependent translocation of sphingosine kinase to the plasma membrane drives its oncogenic signalling. *J Exp Med*. 2005;201(1):49-54.
28. Hengst JA, Guilford JM, Conroy EJ, Wang X, Yun JK. Enhancement of sphingosine kinase 1 catalytic activity by deletion of 21 amino acids from the COOH-terminus. *Arch Biochem Biophys*. 2010;494(1):23-31.
29. Jin HJ, Kim J, Yu J. Androgen receptor genomic regulation. *Transl Androl Urol*. 2013;2(3):157-177.
30. He Y, Lu J, Ye Z, et al. Androgen receptor splice variants bind to constitutively open chromatin and promote abiraterone-resistant growth of prostate cancer. *Nucleic Acids Res*. 2018;46(4):1895-1911.
31. Rana M, Dong J, Robertson MJ, Basil P, Coarfa C, Weigel NL. Androgen receptor and its splice variant, AR-V7, differentially induce mRNA splicing in prostate cancer cells. *Sci Rep*. 2021;11(1):1393.
32. Svensson C, Ceder J, Iglesias-Gato D, et al. REST mediates androgen receptor actions on gene repression and predicts early recurrence of prostate cancer. *Nucleic Acids Res*. 2014;42(2):999-1015.
33. Nagahashi M, Takabe K, Terracina KP, et al. Sphingosine-1-phosphate transporters as targets for cancer therapy. *Biomed Res Int*. 2014;2014:651727.
34. Flores-Morales A, Bergmann TB, Lavallee C, et al. Proteogenomic characterization of patient-derived xenografts highlights the role of REST in neuroendocrine differentiation of castration-resistant prostate cancer. *Clin Cancer Res*. 2019;25(2):595-608.
35. Zhu Y, Liu C, Cui Y, Nadiminty N, Lou W, Gao AC. Interleukin-6 induces neuroendocrine differentiation (NED) through suppression of RE-1 silencing transcription factor (REST). *Prostate*. 2014;74(11):1086-1094.
36. Lin TP, Chang YT, Lee SY, et al. REST reduction is essential for hypoxia-induced neuroendocrine differentiation of prostate cancer cells by activating autophagy signaling. *Oncotarget*. 2016;7(18):26137-26151.
37. Nesti E, Corson GM, McCleskey M, Oyer JA, Mandel G. C-terminal domain small phosphatase 1 and MAP kinase reciprocally control REST stability and neuronal differentiation. *Proc Natl Acad Sci USA*. 2014;111(37):E3929-E3936.
38. Gilani S, Guo CC, Li-Ning EM, Pettaway C, Troncoso P. Transformation of prostatic adenocarcinoma to well-differentiated neuroendocrine tumor after hormonal treatment. *Hum Pathol*. 2017;64:186-190.
39. Spiotto MT, Chung TDK. STAT3 mediates IL-6-induced neuroendocrine differentiation in prostate cancer cells. *Prostate*. 2000;42(3):186-195.
40. Zhang X, Coleman IM, Brown LG, et al. SRRM4 expression and the loss of REST activity may promote the emergence of the neuroendocrine phenotype in castration-resistant prostate cancer. *Clin Cancer Res*. 2015;21(20):4698-4708.
41. Choi SM, Kam SC. Metabolic effects of androgen deprivation therapy. *Korean J Urol*. 2015;56(1):12-18.
42. Wolny-Rokicka E, Tukiendorf A, Wydmanski J, Ostrowska M, Zembron-Lacny A. Lipid status during combined treatment in prostate cancer patients. *Am J Mens Health*. 2019;13(5):1557988319876488.
43. Lin LC, Gao AC, Lai CH, Hsieh JT, Lin H. Induction of neuroendocrine differentiation in castration resistant prostate cancer cells by adipocyte differentiation-related protein (ADRP) delivered by exosomes. *Cancer Lett*. 2017;391:74-82.
44. Blaho VA, Hla T. An update on the biology of sphingosine 1-phosphate receptors. *J Lipid Res*. 2014;55(8):1596-1608.
45. Proia RL, Hla T. Emerging biology of sphingosine-1-phosphate: its role in pathogenesis and therapy. *J Clin Invest*. 2015;125(4):1379-1387.
46. Xu Y, Dong B, Wang J, Zhang J, Xue W, Huang Y. Sphingosine kinase 1 overexpression contributes to sunitinib resistance in clear cell renal cell carcinoma. *Oncoimmunology*. 2018;7(12):e1502130.

47. Grbcic P, Sedic M. Sphingosine 1-phosphate signaling and metabolism in chemoprevention and chemoresistance in colon cancer. *Molecules*. 2020;25(10):2436.
48. Lee CF, Dang A, Hernandez E, et al. Activation of sphingosine kinase by lipopolysaccharide promotes prostate cancer cell invasion and metastasis via SphK1/S1PR4/matriptase. *Oncogene*. 2019;38(28):5580-5598.
49. Visentin B, Vekich JA, Sibbald BJ, et al. Validation of an anti-sphingosine-1-phosphate antibody as a potential therapeutic in reducing growth, invasion, and angiogenesis in multiple tumor lineages. *Cancer Cell*. 2006;9(3):225-238.
50. Balthasar S, Samulin J, Ahlgren H, et al. Sphingosine 1-phosphate receptor expression profile and regulation of migration in human thyroid cancer cells. *Biochem J*. 2006;398(3):547-556.
51. Kalhori V, Törnquist K. MMP2 and MMP9 participate in SIP-induced invasion of follicular ML-1 thyroid cancer cells. *Mol Cell Endocrinol*. 2015;404:113-122.
52. Guo YX, Ma YJ, Han L, Wang YJ, Han JA, Zhu Y. Role of sphingosine 1-phosphate in human pancreatic cancer cells proliferation and migration. *Int J Clin Exp Med*. 2015;8(11):20349-20354.
53. Kim E-S, Kim J-S, Kim SG, Hwang S, Lee CH, Moon A. Sphingosine 1-phosphate regulates matrix metalloproteinase-9 expression and breast cell invasion through SIP3-Gαq coupling. *J Cell Sci*. 2011;124(13):2220-2230.
54. Li MH, Sanchez T, Yamase H, et al. SIP/S1P1 signaling stimulates cell migration and invasion in Wilms tumor. *Cancer Lett*. 2009;276(2):171-179.
55. Shida D, Fang X, Kordula T, et al. Cross-talk between LPA1 and epidermal growth factor receptors mediates up-regulation of sphingosine kinase 1 to promote gastric cancer cell motility and invasion. *Cancer Res*. 2008;68(16):6569-6577.
56. Wang D, Zhao Z, Caperell-Grant A, et al. SIP differentially regulates migration of human ovarian cancer and human ovarian surface epithelial cells. *Mol Cancer Ther*. 2008;7(7):1993-2002.
57. Devine KM, Smicun Y, Hope JM, Fishman DA. SIP induced changes in epithelial ovarian cancer proteolysis, invasion, and attachment are mediated by Gi and Rac. *Gynecol Oncol*. 2008;110(2):237-245.
58. Park KS, Kim MK, Lee HY, et al. SIP stimulates chemotactic migration and invasion in OVCAR3 ovarian cancer cells. *Biochem Biophys Res Commun*. 2007;356(1):239-244.
59. Miller AV, Alvarez SE, Spiegel S, Lebman DA. Sphingosine kinases and sphingosine-1-phosphate are critical for transforming growth factor beta-induced extracellular signal-regulated kinase 1 and 2 activation and promotion of migration and invasion of esophageal cancer cells. *Mol Cell Biol*. 2008;28(12):4142-4151.
60. Dayon A, Brizuela L, Martin C, et al. Sphingosine kinase-1 is central to androgen-regulated prostate cancer growth and survival. *PLoS One*. 2009;4(11):e8048.
61. Wang S, Liang Y, Chang W, Hu B, Zhang Y. Triple Negative breast cancer depends on sphingosine kinase 1 (SphK1)/sphingosine-1-phosphate (S1P)/sphingosine 1-phosphate receptor 3 (S1PR3)/notch signaling for metastasis. *Med Sci Monit*. 2018;24:1912-1923.
62. Wagoner MP, Gunsalus KT, Schoenike B, Richardson AL, Friedl A, Roopra A. The transcription factor REST is lost in aggressive breast cancer. *PLoS Genet*. 2010;6(6):e1000979.
63. Sukocheva O, Wadham C. Role of sphingolipids in oestrogen signalling in breast cancer cells: an update. *J Endocrinol*. 2014;220(3):R25-R35.
64. Gupta P, Khan FI, Roy S, et al. Functional implications of pH-induced conformational changes in the Sphingosine kinase 1. *Spectrochim Acta A Mol Biomol Spectrosc*. 2020;225:117453.
65. Gupta P, Khan FI, Ambreen D, et al. Investigation of guanidinium chloride-induced unfolding pathway of sphingosine kinase 1. *Int J Biol Macromol*. 2020;147:177-186.
66. Khan FI, Gupta P, Roy S, et al. Mechanistic insights into the urea-induced denaturation of human sphingosine kinase 1. *Int J Biol Macromol*. 2020;161:1496-1505.
67. Khan FI, Lai D, Anwer R, Azim I, Khan MKA. Identifying novel sphingosine kinase 1 inhibitors as therapeutics against breast cancer. *J Enzyme Inhib Med Chem*. 2020;35(1):172-186.
68. Beg A, Khan FI, Lobb KA, Islam A, Ahmad F, Hassan MI. High throughput screening, docking, and molecular dynamics studies to identify potential inhibitors of human calcium/calmodulin-dependent protein kinase IV. *J Biomol Struct Dyn*. 2019;37(8):2179-2192.
69. Syed SB, Khan FI, Khan SH, et al. Mechanistic insights into the urea-induced denaturation of kinase domain of human integrin linked kinase. *Int J Biol Macromol*. 2018;111:208-218.

## SUPPORTING INFORMATION

Additional supporting information may be found in the online version of the article at the publisher's website.

**How to cite this article:** Lee C-F, Chen Y-A, Hernandez E, et al. The central role of Sphingosine kinase 1 in the development of neuroendocrine prostate cancer (NEPC): A new targeted therapy of NEPC. *Clin Transl Med*. 2022;12:e695.  
<https://doi.org/10.1002/ctm2.695>